AN EXTENDED CONJUGATE POINT THEORY WITH APPLICATION TO THE STABILITY OF PLANAR BUCKLING OF AN ELASTIC ROD SUBJECT TO A REPULSIVE SELF-POTENTIAL

KATHLEEN A. HOFFMAN * AND ROBERT S. MANNING†

Abstract. The theory of conjugate points in the classic calculus of variations allows, for a certain class of functionals, the characterization of a critical point as stable (i.e., a local minimum) or not. In this work, we generalize this theory to more general functionals, assuming certain generic properties of the second variation operator. The extended conjugate point theory is then applied to a two-dimensional elastic rod subject to pointwise self-repulsion. The critical points are computed by numerically solving first-order integro-differential equations using a finite difference scheme. The stability of each critical point is then computed by determining conjugate points of the second variation operator. In addition, the generalized theory requires the numerical evaluation of the crossing velocity of the zero eigenvalue of the second variation operator at each conjugate point, a feature not present in the classic case (where the crossing velocity can be shown to always be negative). Results demonstrate that the repulsive potential has a stabilizing influence on some branches of critical points.

Key words. Conjugate points, Morse index, constrained variational principles, non-local potential energy

AMS subject classifications. 49K22, 74K10

1. Introduction. The past several decades have seen a surge of interest in continuum elastic rods within the DNA modeling community. Some useful results have been obtained with models that allow the rod to pass through itself, but for DNA longer than a few hundred base-pairs, a model of self-contact is necessary to capture the most important configurations. This self-contact has been modeled via a non-interpenetration constraint ("hard contact"), or, as we do here, via a repulsive self-potential ("soft contact"). The addition of self-contact (in either form), however, significantly increases the complexity of the problem. For instance, with soft contact, the first-order Euler-Lagrange equations become integro-differential equations, rather than the standard second-order differential equations. And, most pertinent to this article, classic techniques regarding the second variation and stability analysis no longer apply.

Here we assume the existence of local minimizers of the elastic-plus-contact energy. Existence of minima for the hard contact model has been addressed by Gonzalez et al [6], Strzelecki [23], and Schuricht et al [22]. Existence of minima for the soft contact model was addressed by Hoffman and Seidman [13].

This article focuses on developing a theory and associated computations to determine which critical points (equilibria) of the energy are local minima (stable), by exploiting the variational structure of the formulation. In unconstrained calculus of variations theory, there are necessary and sufficient conditions for a critical point to be a local minimum that involve the condition that the second variation evaluated at that critical point does not have any conjugate points. This idea of a conjugate point was first developed by Jacobi (see, e.g., the texts [4, 5, 11, 20]), and was subsequently generalized to the idea of an "index" of a critical point by Morse and others [18, 9]. In the presence of isoperimetric constraints, Bolza [2], citing work of Weierstrass, de-

*Department of Mathematics and Statistics; University of Maryland, Baltimore County; Baltimore, MD 21250 (khoffman@math.umbc.edu)

†Mathematics Department; Haverford College; Haverford, PA 19041 (rmanning@haverford.edu)

veloped a necessary condition for a critical point to be a constrained minimum, which exactly corresponds to an analogous definition of conjugate point in the constrained setting. This idea was further pursued by Manning, Rogers and Maddocks [17] and linked to the value of a constrained index. In this paper, we follow the formulation of [17] to develop an index theory for more general functionals, including calculus of variations problems with a non-local potential term, focusing in particular on the example of a self-repulsive energy for a planar rod.

Among the considerable literature on rods with self-contact, a small minority of studies focus on the question of stability that we address here. Van der Heijden et al [28] look at jump phenomena in bifurcation diagrams as evidence of loss of stability, but without proposing specific stability tests per se. Tobias, Swigon, and Coleman [27, 3] develop stability tests for a homogeneous intrinsically straight 3D rod with a quite general contact energy. Their tests involve conditions on branches of solutions, focusing in particular on the link-writhe bifurcation diagram. Our approach here will be quite different in several ways. We focus on a test that is applied to a single critical point, rather than a condition that compares a critical point to nearby critical points. We also propose a specific algorithm for determining stability (akin to solving the Jacobi equations in the calculus of variations), applicable to a quite general elastic energy, including, for example, intrinsic shape.

Our numerical computations for the planar rod involve straightforward finite differences combined with parameter continuation. This example provides a simple illustration of the stability theory that is the focus of this article. More intricate numerical approaches have been applied to the 3D version of this problem [30, 27, 3, 24, 26] (or the 3D dynamical problem [15, 8, 7]), and our stability test should extend easily to the 3D setting, though of course requiring similarly more intense numerics.

2. General Formulation. Here we sketch the general outline of an extended conjugate point theory. The presentation is purposefully vague (we do not write a specific form for the functional of interest, and omit complete definitions of terms like "admissible variation", "first variation", or "second variation"), so as to quickly convey the basic approach. In the rest of the paper, we apply this approach to specific problems, first to the classic calculus of variations problem in Sec. 3 and then to a planar rod model with self-repulsive energy in Sec. 4.

Consider the problem of minimizing a real-valued functional J defined on a set $\mathsf{D}([a,b])$ of L^2 functions on an interval $[a,b]$. Given $\mathsf{D}([a,b])$, there is a corresponding vector space $\mathsf{A}([a,b])$ of "admissible variations", which consists of those functions h such that if y is in $\mathsf{D}([a,b])$, so is $y+h$, at least to first order in h. This space $\mathsf{A}([a,b])$ is equipped with the L^2-norm $\|\ \|$.

We further assume that for each $y \in \mathsf{D}([a,b])$, J is twice differentiable at y, i.e., for each admissible variation $h \in \mathsf{A}([a,b])$, we have $J[y+h] - J[y] = \delta J[h] + \delta^2 J[h] + \epsilon[h]\|h\|^2$ where δJ is a linear functional from $\mathsf{A}([a,b])$ to $\mathbb{R}$ (called the *first variation*), $\delta^2 J$ is a quadratic functional from $\mathsf{A}([a,b])$ to $\mathbb{R}$ (called the *second variation*), and ϵ is a functional from $\mathsf{A}([a,b])$ to $\mathbb{R}$ such that $\epsilon \to 0$ as $h \to 0$ (cf. [5, pp. 97–99] for more on this setup within the standard calculus of variations setting). A necessary condition for y to be a local minimizer of J is that $\delta J[h] = 0$ for all $h \in \mathsf{A}([a,b])$. Functions that satisfy this condition will be called *critical points*.

Further assume that on a subspace $\tilde{\mathsf{A}}([a,b])$ of $\mathsf{A}([a,b])$, the second variation can be written as a quadratic form $\delta^2 J[h] = \langle h, \mathcal{S}h\rangle$, where $\mathcal{S} : \tilde{\mathsf{A}}([a,b]) \to L^2([a,b])$ is called the *second-variation operator*, and $\langle\cdot,\cdot\rangle$ denotes the standard L^2 inner product. (As will be illustrated in the next section, the invocation of a new subspace $\tilde{\mathsf{A}}$ at

this point usually arises because the definition of A does not require h to have two derivatives, whereas $\mathcal{S}$ is a second-order differential operator.)

Finally, assume that $\tilde{\mathsf{A}}([a,b])$ and $\mathsf{A}([a,b])$ are dense in a space $\mathsf{W}([a,b])$ that contains the range of $\mathcal{S}$. In that case, we can study the spectrum of $\mathcal{S} : \mathsf{W}([a,b]) \to \mathsf{W}([a,b])$ (densely defined on $\tilde{\mathsf{A}}([a,b])$), and the properties of this spectrum will determine the behavior of the second variation on $\mathsf{A}([a,b])$.

Specifically, for each critical point, we would like to assign an index, a non-negative integer that measures the dimension of the space on which the second variation is negative, i.e., the number of negative eigenvalues of $\mathcal{S}$ on $\tilde{\mathsf{A}}([a,b])$. To this end, we embed the space $\tilde{\mathsf{A}}([a,b])$ in a family of spaces $\tilde{\mathsf{A}}([a,\sigma])$ as σ varies from a to b, and similarly embed the operator $\mathcal{S}$ within a family of operators $\mathcal{S}_\sigma$ (where $\tilde{\mathsf{A}}([a,\sigma])$ is dense in a space that contains the range of $\mathcal{S}_\sigma$), and consider the following family of eigenvalue problems:

$$\mathcal{S}_\sigma h = \rho(\sigma) h, \quad h \in \tilde{\mathsf{A}}([a,\sigma]). \tag{2.1}$$

Now assume that for our chosen family of spaces $\tilde{\mathsf{A}}([a,\sigma])$ and operators $\mathcal{S}_\sigma$, we have the following properties about the family of spectra $\rho(\sigma)$:

A1: The spectrum of each $\mathcal{S}_\sigma$ consists of isolated simple eigenvalues

$$-\infty < \rho_1(\sigma) < \rho_2(\sigma) < \cdots$$

A2: The eigenvalues $\rho_n(\sigma)$ are continuously dependent on σ.

A3: The functions $\rho_n(\sigma)$ never have a turning point at $\rho = 0$, i.e., if $\rho_n(\sigma^*) = 0$, then $\rho_n(\sigma)$ has one sign just to the left of σ^* and the other sign just to the right. One might informally call this a "transverse crossing condition".

A4: For σ sufficiently close to a, the number of negative eigenvalues of $\mathcal{S}_\sigma$ is known.

Within this structure, we define conjugate points to be values of σ such that the equation

$$\mathcal{S}_\sigma h = 0, \quad h \in \tilde{\mathsf{A}}([a,\sigma]) \tag{2.2}$$

has a nontrivial solution h. The values of σ that are conjugate points exactly correspond to the values of σ for which $\mathcal{S}_\sigma$ has a zero eigenvalue, i.e. $\rho(\sigma) = 0$. Further, by assumption **A3**, either ρ goes from negative to positive as σ increases (a case we will call "positive velocity") or ρ goes from positive to negative as σ increases ("negative velocity"). The index measures the size of the space on which the second variation is negative and this exactly corresponds to the number of negative eigenvalues of $\mathcal{S}_\sigma$ at $\sigma = b$. The combination of properties $\mathbf{A1} - \mathbf{A3}$ means that we can relate the index to the number of conjugate points through the following principle:

Index Principle: The index of a critical point can be computed according to:

$$\begin{aligned}\text{Index} = &\left(\begin{array}{c}\text{the number of negative eigenvalues of } \mathcal{S}_\sigma \\ \text{for } \sigma \text{ sufficiently close to } a\end{array}\right) \\ &+\left(\begin{array}{c}\text{number of conjugate points in the interval} \\ a<\sigma<b \text{ with negative velocity}\end{array}\right) \\ &-\left(\begin{array}{c}\text{number of conjugate points in the interval} \\ a<\sigma<b \text{ with positive velocity}\end{array}\right).\end{aligned} \tag{2.3}$$

Thus, if one can determine the number of negative eigenvalues that $\mathcal{S}_\sigma$ starts with (for σ sufficiently close to a), as assumed in **A4**, then the index can be computed by tracking conjugate points and their crossing velocities.

Before proceeding to our two examples, we preview what we will show about **A1** – **A4** in each case. For the classic problem in the calculus of variations (Sec. 3), all of **A1** – **A4** can be proven. Specifically, the fact that $\mathcal{S}_\sigma$ is a Sturm-Liouville operator obeying Legendre's strengthened condition leads to **A1**, **A2**, and **A4**, and an argument based on a variational characterization of the eigenvalues shows that they are decreasing functions of σ, thus trivially verifying **A3**.

In extending the theory to a wider class of problems, such as we do in the planar rod example in Sec. 4, we may need to settle for some parts of **A1** – **A4** to remain as assumptions rather than provable properties. Specifically, **A3**, and the part of **A1** that says that the eigenvalues are simple, are two properties that may fail when the classic second variation operator is perturbed, because the perturbation could merge two previously distinct eigenvalues, and could (and does in our example) create turning points in $\rho(\sigma)$, which could in principle occur at a zero eigenvalue. It seems clear that a *generic* perturbation will not cause either of these failures (an exact coalescence of eigenvalues, or a turning point exactly at zero). This allows one to apply the generalized theory with some confidence, even if these particular properties are difficult to prove. In our planar rod example, we prove **A2**, **A4**, and **A1** without the "simple" condition, and also argue that our numerical implementation should show signs of a (non-generic) violation of **A3** or non-simple eigenvalues.

3. Example: The classic problem in the calculus of variations. Consider the functional

$$J[q] = \int_0^1 L(q(s), q'(s), s)\, ds, \tag{3.1}$$

which we would like to minimize over all $q \in C^1([0,1])$ that obey the boundary conditions

$$q(0) = q_L, \quad q(1) = q_R \tag{3.2}$$

for some given q_L, q_R. The corresponding set of admissible variations is

$$\mathsf{A}([0,1]) \equiv \left\{h \in C^1([0,1]) : h(0) = 0,\ h(1) = 0\right\}.$$

If we assume that L is C^3 in its arguments, then we can Taylor-expand to second-order inside the integral to show that J is a twice-differentiable functional. As described in Sec. 2, critical points are defined by the condition that the first variation vanishes. In this setting they are solutions of the Euler-Lagrange equations

$-\frac{d}{ds}(L_{q'}) + L_q = 0$ (subscripting by q or q' denotes partial differentiation) that also satisfy the boundary conditions in (3.2). Classification of a given critical point q involves an analysis of the second variation of (3.1) (at q), which, by integration by parts, can be rewritten on the subspace

$$\tilde{\mathsf{A}}([0,1]) \equiv \left\{h \in C^2([0,1]) : h(0) = 0,\ h(1) = 0\right\}$$

as

$$\delta^2 J[h] = \frac{1}{2}\int_0^1 h(s)(\mathcal{S}h)(s)\, ds,$$

where $\mathcal{S}$ is the second-order differential operator:

$$\mathcal{S}h \equiv -\frac{d}{ds}\left[Ph'\right] + (Q - C')h, \tag{3.3}$$

and $P(s) \equiv L_{q'q'}(q(s))$, $C(s) \equiv L_{qq'}(q(s))$, and $Q(s) \equiv L_{qq}(q(s))$. We assume Legendre's strengthened condition: $P(s) > 0$ for all $s \in [0,1]$.

We define $\mathsf{W}([0,1]) = L^2([0,1])$ (which clearly contains the range of $\mathcal{S}$), and note that $\tilde{\mathsf{A}}([0,1])$ and $\mathsf{A}([0,1])$ are dense in $\mathsf{W}([0,1])$, as required by our presentation of the general theory.

We make the following natural choice for embedding $\tilde{\mathsf{A}}([0,1])$ in a family of spaces:

$$\tilde{\mathsf{A}}([0,\sigma]) \equiv \left\{h \in C^2([0,\sigma]) : h(0) = 0,\ h(\sigma) = 0\right\},$$

and let $\mathcal{S}_\sigma = \mathcal{S}$ for each σ. With $\mathsf{W}([0,\sigma]) = L^2([0,\sigma])$, we apply the general theory from Sec. 2, and find that in this setting, a conjugate point is a value $\sigma < 1$ for which there is a nontrivial solution to:

$$(\mathcal{S}h)(s) = 0 \text{ for } 0 < s < \sigma,\ \ h(0) = 0,\ h(\sigma) = 0. \tag{3.4}$$

This definition of conjugate point is equivalent to Jacobi's classical definition of conjugate point (see, for example, [11, p.124]).

In order to justify the conjugate point theory, we establish assumptions **A1** $-$ **4** for the family of eigenvalue problems

$$(\mathcal{S}h)(s) = \rho(\sigma)h(s) \text{ for } 0 < s < \sigma,\ \ h(0) = 0,\ h(\sigma) = 0. \tag{3.5}$$

Since $\mathcal{S}$ is a Sturm-Liouville operator satisfying Legendre's strengthened condition, and since the boundary conditions imposed are separated and self-adjoint, **A1** is known to hold (see, e.g., [31, p. 5]). In addition, **A2** has been proven by Kong and Zettl [31, p. 7][1]. In an earlier paper, we verified **A3** using Rayleigh quotients and other techniques [17]; more specifically, $\rho_n(\sigma)$ is a decreasing function (so that all conjugate points are of "negative velocity" type, in the sense described in Sec. 2).

Finally, we verify **A4**, showing specifically that all eigenvalues are positive for $\sigma > 0$ small. First we reformulate the eigenvalue problems so that they involve a

[1] As discussed in Remark 3.1 of [31], Kong and Zettl prove that each eigenvalue ρ_i lies on a continuous branch, but point out that this does not in general imply that for a fixed n, ρ_n is always continuous, since a new eigenvalue can appear from $-\infty$. However, this cannot happen for our example since there exists a uniform lower bound for the eigenvalues, as can be seen via our verification of **A4**. Alternatively, our proof of **A2** for the planar rod example in Sec. 4, which exploits a variational formula for ρ_n, could be adapted to prove **A2** in this setting as well.

fixed function space, via the change of variables $t = s/\sigma$, which yields the following equivalent formulation of (3.5):

$$(\mathcal{S}_\sigma h)(t) = \rho(\sigma)h(t) \text{ for } 0 < t < 1, \;\; h(0) = 0, \; h(1) = 0$$

where

$$\mathcal{S}_\sigma h(t) \equiv -\frac{1}{\sigma^2}\frac{d}{dt}\left[P(\sigma t)h'(t)\right] - \left(Q(\sigma t) - C'(\sigma t)\right)h(t). \tag{3.6}$$

We first analyze the spectrum of the first half of this operator:

$$\mathcal{T} \equiv -\frac{1}{\sigma^2}\frac{d}{dt}\left[P(\sigma t)\frac{d}{dt}\right].$$

We take the eigenvalue problem

$$-\frac{d}{dt}\left[P(\sigma t)h'(t)\right] = \rho h(t)$$

and multiply both sides by $h(t)$, integrate from 0 to 1, and integrate the left side by parts to see that

$$\rho\|h\|^2 = \langle h', P(\sigma t)h'\rangle.$$

By Legendre's strengthened condition, the right-hand side is positive, and thus so must be the eigenvalues of the operator $-d/dt[P(\sigma t)d/dt]$, call them $\lambda_1 < \lambda_2 < \cdots$. Therefore, the eigenvalues of $\mathcal{T}$ are $\lambda_1/\sigma^2 < \lambda_2/\sigma^2 < \cdots$. The operator $\mathcal{S}_\sigma$ is $\mathcal{T}$ plus a "perturbation" (multiplication by $(Q(\sigma t) - C'(\sigma t))$), which is bounded with

$$\|Q(\sigma t) - C'(\sigma t)\| \leq ||Q||_\infty + ||C'||_\infty. \tag{3.7}$$

Kato [14, Thm 4.10, p. 291] shows that every eigenvalue in the spectrum of $\mathcal{S}_\sigma$ is within $\|Q(\sigma t) - C'(\sigma t)\|$ of an eigenvalue in the spectrum of $\mathcal{T}$. Since our bound on the perturbation in (3.7) is independent of σ, and the lowest eigenvalue of $\mathcal{T}$ is λ_1/σ^2 with $\lambda_1 > 0$, the eigenvalues of $\mathcal{S}_\sigma$ will be positive for σ sufficiently close to zero.

Since the eigenvalues are all positive for $\sigma \approx 0$ and all conjugate points are of "negative velocity", the general index principle takes on the following simpler form:

$$\text{Index} = \left(\begin{array}{c}\text{number of conjugate points in the interval} \\ 0 < \sigma < 1 \text{ (which all have negative velocity)}\end{array}\right). \tag{3.8}$$

This is exactly Morse's classic result [18], and includes as a special case the classic "Jacobi's necessary condition", that in order for a critical point to be a local minimum (i.e., the index is zero), there must be no conjugate points.

This paper presents a generalization of the classical Jacobi conjugate point theory embodied in this example. We assume merely that the second variation operator $\mathcal{S}$ satisfies assumptions **A1**–**A4**, rather than require it to take the usual second-order differential form (3.3), and we use the general index principle (2.3), rather than the specific Morse principle (3.8), which holds only in the special situation that the eigenvalues are monotonically decreasing functions of σ and that all the eigenvalues are positive for σ sufficiently close to a. These generalizations significantly expand the type of problems for which the conjugate point technique can be used.

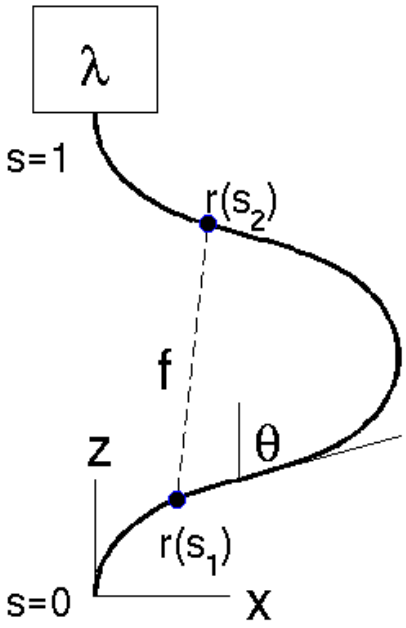

FIG. 4.1. *A planar elastic rod. One end of the rod is at the origin, and the other end is required to be somewhere on the positive z-axis. The direction of the tangent vector to the rod at each point is measured by the angle θ, which is required to be zero at both ends. A load of size λ is imposed on the top of the rod. In addition to elastic forces, each point on the rod experiences a repulsive force f from every other point on the rod (mollified so as to cause f → 0 as s2 → s1).*

4. Example: planar elastic rod subject to self-repulsion.

4.1. Variational Formulation. Consider the following model for the elastic energy of a planar elastic rod subject to a vertical endload λ and self-repulsion described by a potential function f (see Fig. 4.1):

$$J = \int_0^1 \left\{ \frac{K}{2}(\theta'(s) - \hat{\theta}'(s))^2 + \lambda \cos\theta(s) + \int_0^1 f(|s-t|, |\mathbf{r}(s) - \mathbf{r}(t)|)dt \right\} ds, \quad (4.1)$$

Here, the position $\mathbf{r} = (x, z)$ of the rod in the xz-plane is described as a function of an arclength parameter s, with units chosen so the total arclength is one. The function $\theta(s)$ is the tilt angle of the tangent vector to the rod, i.e.,

$$\frac{d\mathbf{r}}{ds} = \mathbf{d}_3(\theta) \equiv (\sin\theta, \cos\theta), \quad (4.2)$$

(we use the notation $\mathbf{d}_3$ to be consistent with a standard formulation of a three-dimensional elastic rod, where (4.2) is an inextensibility-unshearability constraint relating the tangent vector of the centerline to the normal vector of the rod cross-section). This relationship implies that $\mathbf{r}$ can be determined from θ, via

$$\mathbf{r}(s) = \int_0^s \mathbf{d}_3(\theta(w))dw, \tag{4.3}$$

so that J is in fact a functional of only $\theta(s)$.

The first term in (4.1) describes bending energy, with a "stiffness" parameter K and a known function $\hat{\theta}(s)$ that describes the intrinsic shape of the rod. Thus, we are assuming linear elasticity, or a quadratic energy dependence on $\theta' - \hat{\theta}'$, but the index theory and numerical computations could easily be adapted for more general elasticity assumptions. In our examples, we will assume the rod is intrinsically straight, so that $\hat{\theta} \equiv 0$, although in fact our intermediate computations will use nonzero $\hat{\theta}$ as a mechanism for breaking symmetry in order to access branches of buckled configurations.

The second term represents the gravitational potential energy of the endload, because we have $\cos\theta(s) = z'(s)$ by (4.2), so that the integral of $\lambda\cos(\theta(s))$ equals $\lambda[z(1) - z(0)]$, the endload (in weight units) times its height.

The third term in (4.1) represents repulsion between each pair of points on the rod, with potential energy density f. Although the specific form of f is not particularly important to the theory, or the computation, the examples in this paper were computed with

$$f(\chi, \eta) = \left(\frac{\chi e^{7\chi^2}}{1 + \chi e^{7\chi^2}}\right)^4 \frac{a}{\eta},$$

i.e., a repulsive energy potential inversely proportional to separation distance (recall that η denotes $|\mathbf{r}(s) - \mathbf{r}(t)|$ within the functional J), with proportionality constant a, and a "mollifier" (the first term) designed to make the repulsive energy between points at arclength s and t be close to zero for $s \approx t$. The term in parentheses is approximately χ for $\chi \approx 0$ (i.e., $s \approx t$, since $\chi = |s - t|$ will be plugged into f), and is approximately 1 for larger χ (i.e., for points s and t separated along the rod); see Fig. 4.2. This is raised to the fourth power, in order to dominate the power on η in the denominator as $\eta \to 0$ even when two η derivatives are taken within the second variation of J.

We impose the boundary conditions that the rod has one end clamped at the origin and the other end allowed to slide along the z-axis:

$$\theta(0) = \theta(1) = 0, \;\; \mathbf{r}(0) = (0, 0), \;\; \mathbf{r}(1) = (0, *). \tag{4.4}$$

Translating into constraints on θ only, the constraints on $\mathbf{r}$ can be reduced to the single integral constraint $\int_0^1 \sin(\theta(s))ds = 0$, since $\sin(\theta(s)) = x'(s)$, and we need $x(1) - x(0) = 0$.

Thus, we would like to minimize the functional (4.1) (with $\mathbf{r}(s)$ replaced by $\int_0^s \mathbf{d}_3(\theta(w))dw$), over all functions $\theta(s)$ satisfying the boundary conditions $\theta(0) = \theta(1) = 0$ and the integral constraint $\int_0^1 \sin(\theta(s))\, ds = 0$. In the next section we will derive the equilibrium equations for a critical point and describe an algorithm for computing their solution. Sec. 4.4 will describe how the theory in Sec. 2 can be used to compute the index for each critical point.

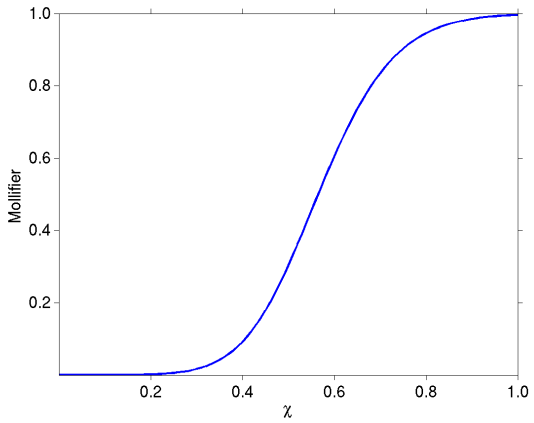

FIG. 4.2. *A graph of the mollifier function* $\left(\frac{\chi e^{7\chi^2}}{1+\chi e^{7\chi^2}}\right)^4$*; this multiplies the one-over-distance term in the repulsive energy potential* f *that appears in (4.1). The expression* $|s-t|$ *is plugged in for* χ *within the potential; hence, a value of* $\chi \approx 0$ *represents a pair of points on the rod that are very close in arclength, while a larger value of* χ *represents a pair of points that are distant in arclength.*

4.2. The First Variation and Equilibrium Equations.

4.2.1. Derivation. In this section, we derive the first variation of J and set $\delta J = 0$ to obtain the equilibrium equations. We substitute $\theta(s) + h(s)$ into (4.1), recalling that $\mathbf{r}(s)$ is related to $\theta(s)$ via (4.3), and collect the first-order terms in h:

$$\delta J[h] = \int_0^1 \left[K[\theta'(s) - \hat{\theta}'(s)]h'(s) - \lambda \sin(\theta(s))h(s)\right] ds \tag{4.5}$$
$$+ \int_0^1 \int_0^1 \frac{f_\eta(|s-t|, |\mathbf{r}(s) - \mathbf{r}(t)|)}{|\mathbf{r}(s) - \mathbf{r}(t)|} (\mathbf{r}(s) - \mathbf{r}(t))^T \int_t^s h(w)(\mathbf{d}_3)_\theta(\theta(w)) dw\, dt\, ds,$$

where the θ and η subscripts indicate differentiation. Similarly, we substitute into the boundary conditions (4.4) and the integral constraint in order to find the "linearized" boundary conditions and constraints to be applied to h:

$$h(0) = h(1) = 0, \quad \int_0^1 \cos(\theta(s))h(s)ds = 0. \tag{4.6}$$

Next, we write $\delta J[h]$ as an L^2 inner product $\delta J[h] = \langle h, X\rangle$ for some function X, using the following lemma.

LEMMA 4.1. *If* $\mathbf{G}(s,t)$*,* $\mathbf{H}(s)$ *are vector functions and* $\mathbf{G}(t,s) = -\mathbf{G}(s,t)$ *for all* s, t*, then*

$$\int_0^1 \int_0^1 \int_t^s \mathbf{G}(s,t)^T \mathbf{H}(w) dw dt ds = 2 \int_0^1 \int_s^1 \int_0^1 \mathbf{G}(w,t)^T \mathbf{H}(s) dt dw ds$$

Proof. Let I be the left-hand side and swap the inner two integrals:

$$I = \int_0^1 \int_0^s \int_0^w \mathbf{G}(s,t)^T \mathbf{H}(w) dt dw ds - \int_0^1 \int_s^1 \int_w^1 \mathbf{G}(s,t)^T \mathbf{H}(w) dt dw ds.$$

Next we swap the outer two integrals and then switch the dummy variable names s and w:

$$I = \int_0^1 \int_s^1 \int_0^s \mathbf{G}(w,t)^T \mathbf{H}(s) dt dw ds - \int_0^1 \int_0^s \int_s^1 \mathbf{G}(w,t)^T \mathbf{H}(s) dt dw ds.$$

Next, we note that the (w,t) integration regions of these two integrals are mirror images with respect to the 45-degree line, and thus, since $\mathbf{G}$ is antisymmetric, the two integrals are in fact opposites, so that

$$I = 2 \int_0^1 \int_s^1 \int_0^s \mathbf{G}(w,t)^T \mathbf{H}(s) dt dw ds.$$

Finally, since the integrand is antisymmetric with respect to swapping t and w, its integral over the region $\int_0^1 \int_s^1 \int_s^1 dt\, dw\, ds$ is zero, since that region is symmetric with respect to swapping t and w. We add this zero integral to I to arrive at the desired final form.□

Now, we integrate the first term of (4.5) by parts and apply Lemma 4.1 to the second term, with $\mathbf{G}(s,t) = \frac{f_\eta(|s-t|,|\mathbf{r}(s)-\mathbf{r}(t)|)}{|\mathbf{r}(s)-\mathbf{r}(t)|}(\mathbf{r}(s)-\mathbf{r}(t))$ and $\mathbf{H}(w) = h(w)(\mathbf{d}_3)_\theta(\theta(w))$:

$$\begin{aligned}\delta J[h] = &\int_0^1 \left[-K[\theta''(s) - \hat{\theta}''(s)]h(s) - \lambda \sin\theta(s) h(s)\right] ds \\ &+2\int_0^1 \int_s^1 \int_0^1 h(s) \frac{f_\eta(|w-t|,|\mathbf{r}(w)-\mathbf{r}(t)|)}{|\mathbf{r}(w)-\mathbf{r}(t)|}(\mathbf{r}(w)-\mathbf{r}(t))^T(\mathbf{d}_3)_\theta(\theta(s)) dt\, dw\, ds\end{aligned}$$

Then, $\delta J[h] = \langle h, X\rangle$, where

$$\begin{aligned}X(s) \equiv &-K[\theta''(s) - \hat{\theta}''(s)] - \lambda \sin\theta(s) \\ &+ 2\int_s^1 \int_0^1 \frac{f_\eta(|w-t|,|\mathbf{r}(w)-\mathbf{r}(t)|)}{|\mathbf{r}(w)-\mathbf{r}(t)|}(\mathbf{r}(w)-\mathbf{r}(t))^T(\mathbf{d}_3)_\theta(\theta(s)) dt\, dw.\end{aligned}$$

A critical point is defined by the condition that $\delta J[h] = 0$ for all h satisfying (4.6), so that $\langle h, X\rangle = 0$ for all h with $\langle h, \cos\theta\rangle = 0$. Thus, X is a multiple of $\cos\theta$, so that

$$\begin{aligned}0 = &-K[\theta''(s) - \hat{\theta}''(s)] - \lambda \sin\theta(s) - \mu\cos\theta(s) \\ &+ 2\int_s^1 \int_0^1 \frac{f_\eta(|w-t|,|\mathbf{r}(w)-\mathbf{r}(t)|)}{|\mathbf{r}(w)-\mathbf{r}(t)|}(\mathbf{r}(w)-\mathbf{r}(t))^T(\mathbf{d}_3)_\theta(\theta(s)) dt\, dw.\end{aligned} \tag{4.7}$$

If we define

$$\mathbf{n}(s) \equiv 2\int_s^1 \int_0^1 \frac{f_\eta(|w-t|,|\mathbf{r}(w)-\mathbf{r}(t)|)}{|\mathbf{r}(w)-\mathbf{r}(t)|}(\mathbf{r}(w)-\mathbf{r}(t)) dt\, dw + \begin{bmatrix}-\mu \\ \lambda\end{bmatrix},$$

then our equilibrium equations are:

$$\begin{aligned}\mathbf{n}(s)^T(\mathbf{d}_3)_\theta(\theta(s)) &= K[\theta'' - \hat{\theta}''], \\ \mathbf{n}'(s) &= -2\int_0^1 f_\eta(|s-t|,|\mathbf{r}(s)-\mathbf{r}(t)|)\frac{\mathbf{r}(s)-\mathbf{r}(t)}{|\mathbf{r}(s)-\mathbf{r}(t)|} dt, \\ \mathbf{r}'(s) &= \mathbf{d}_3(\theta(s)),\end{aligned} \tag{4.8}$$

subject to the boundary conditions $\theta(0) = 0$, $\theta(1) = 0$, $x(0) = 0$, $x(1) = 0$, $z(0) = 0$, and $n_z(1) = \lambda$ (which follows from the definition of $\mathbf{n}$; note that we don't consider the condition $n_x(1) = -\mu$ as a boundary condition, since μ is an unknown constant).

4.2.2. Computing Critical Points. The equilibrium equations (4.9) are a set of integro-differential equations that can be solved using a standard finite difference method. Subdivide $[0,1]$ into N equal pieces of length $\Delta s = \frac{1}{N}$ and let $\mathbf{z}_i$ be our approximation for the value of $\mathbf{z}(\frac{i}{N})$. The approximation of the equilibrium equations at $s = \frac{i}{N}$ is:

$$\begin{aligned}
&\mathbf{n}_i^T(\mathbf{d}_3)_\theta(\theta_i) = K\frac{\theta_{i+1} - 2\theta_i + \theta_{i-1}}{(\Delta s)^2} - K\hat{\theta}''(i/n), \quad i = 1,\dots,N-1 \\
&\frac{\mathbf{n}_i - \mathbf{n}_{i-1}}{\Delta s} = -2\sum_{j=0,j\neq i}^{N-1}\left[f_\eta\left(\left|\frac{i}{N} - \frac{j}{N}\right|, |\mathbf{r}_i - \mathbf{r}_j|\right)\frac{\mathbf{r}_i - \mathbf{r}_j}{|\mathbf{r}_i - \mathbf{r}_j|}\right]\frac{\Delta s}{2} \\
&\quad - 2\sum_{j=0,j\neq i-1}^{N-1}\left[f_\eta\left(\left|\frac{i}{N} - \frac{j+1}{N}\right|, |\mathbf{r}_i - \mathbf{r}_{j+1}|\right)\frac{\mathbf{r}_i - \mathbf{r}_{j+1}}{|\mathbf{r}_i - \mathbf{r}_{j+1}|}\right]\frac{\Delta s}{2}, \quad i = 1,\dots,N, \\
&\frac{\mathbf{r}_i - \mathbf{r}_{i-1}}{\Delta s} = \mathbf{d}_3(\theta_i), \quad i = 1,\dots,N,
\end{aligned} \tag{4.9}$$

where the integral has been approximated using a trapezoid rule. There are $5N-1$ unknowns, namely $\theta_1,\dots\theta_{N-1}$, $\mathbf{r}_1,\dots,\mathbf{r}_{N-1}$, z_N, $\mathbf{n}_0,\dots,\mathbf{n}_{N-1}$, and $(n_x)_N$ to be determined from the $5N-1$ equations in (4.9). The remaining variables θ_0, θ_N, $\mathbf{r}_0$, x_N, and $(n_z)_N$ are known from the boundary conditions.

The system of equations (4.9) were solved via parameter continuation in λ using the Trilinos package [10] (`http://trilinos.sandia.gov`), using the NOX package [19] to solve the nonlinear system and LOCA [21] to control the parameter continuation. See Sec. 4.5 for further details.

4.3. The Second Variation. To assign an index to each critical point, the second variation is computed and expressed as a quadratic form. We have previously shown in [17] how the general theory presented in Sec. 2 implies that the presence of an isoperimetric constraint (here $\int_0^1 \sin(\theta(s))ds = 0$) leads to the inclusion of a familiar Lagrange multiplier term in the second variation: we replace the functional J from (4.1) by $J^* \equiv J - \mu\int_0^1 \sin\theta(s)ds$ for some constant μ and then apply the standard conjugate point theory to $\delta^2 J^*$ (cf. [11, p. 85]).

We substitute $\theta + h$ into the functional J^* and collect the terms of second-order in h. After an integration by parts, we find:

$$\delta^2 J^*[h] = \frac{1}{2}\int_0^1 h(s)(-Kh''(s) - \lambda\cos\theta(s)h(s) + \mu\sin\theta(s)h(s))ds + R[h], \tag{4.10}$$

where $R[h]$ is the piece coming from the repulsive potential term:

$$\begin{aligned}
R[h] = \frac{1}{2}\int_0^1\int_0^1 \Bigg\{ &\left(\int_t^s (\mathbf{d}_3)_\theta(\tau)h(\tau)d\tau\right)^T \mathbf{M}(s,t)\left(\int_t^s (\mathbf{d}_3)_\theta(\kappa)h(\kappa)d\kappa\right) \\
&+ \int_t^s \left[f_\eta(|s-t|,|\mathbf{x}|)\frac{\mathbf{x}^T}{|\mathbf{x}|}\right]h(w)^2(\mathbf{d}_3)_{\theta\theta}(w)dw\Bigg\}dtds,
\end{aligned}$$

for $\mathbf{x} \equiv \mathbf{r}(s) - \mathbf{r}(t)$ and the 2×2 matrix function $\mathbf{M}$ defined by

$$\mathbf{M}(s,t) \equiv \left[f_{\eta\eta}(|s-t|,|\mathbf{x}|)\frac{\mathbf{x}\mathbf{x}^T}{|\mathbf{x}|^2} + f_\eta(|s-t|,|\mathbf{x}|)\frac{\mathbf{I}}{|\mathbf{x}|} - f_\eta(|s-t|,|\mathbf{x}|)\frac{\mathbf{x}\mathbf{x}^T}{|\mathbf{x}|^3}\right]. \tag{4.11}$$

We note that h lies in the space of admissible variations defined by the linearized boundary conditions and isoperimetric constraint:

$$\tilde{\mathsf{A}}([0,1]) \equiv \left\{ h \in C^2(0,1) : h(0) = h(1) = 0, \quad \int_0^1 \cos(\theta(s))h(s)\, ds = 0 \right\}. \qquad (4.12)$$

Applying Lemma 4.1 to the second half of $R[h]$ with $\mathbf{G}(s,t) = \frac{f_\eta(|s-t|,|\mathbf{r}(s)-\mathbf{r}(t)|)}{|\mathbf{r}(s)-\mathbf{r}(t)|}(\mathbf{r}(s)-\mathbf{r}(t))$ and $\mathbf{H}(w) = h(w)^2(\mathbf{d}_3)_{\theta\theta}(\theta(w)$, we find:

$$R[h] = \int_0^1 \int_s^1 \int_0^1 \left[f_\eta(|w-t|,|\mathbf{r}(w)-\mathbf{r}(t)|)\frac{(\mathbf{r}(w)-\mathbf{r}(t))^T}{|\mathbf{r}(w)-\mathbf{r}(t)|} \right] h(s)^2(\mathbf{d}_3)_{\theta\theta}(s)dtdwds + Z.$$

where

$$Z \equiv \frac{1}{2}\int_0^1 \int_0^1 \int_t^s \int_t^s h(\tau)h(\kappa)(\mathbf{d}_3)_\theta(\tau)^T\mathbf{M}(s,t)(\mathbf{d}_3)_\theta(\kappa)d\tau d\kappa dtds.$$

Inserting this into (4.10), and recalling the definition of $\mathbf{n}$:

$$\delta^2 J^*[h] = \frac{1}{2}\int_0^1 h(s)\left(-Kh''(s) + \mathbf{n}(s)^T(\mathbf{d}_3)_{\theta\theta}(\theta(s))h(s)\right) ds + Z.$$

Given a critical point $(\mathbf{n},\theta,\mathbf{r})$, we give a label to the "Lagrange multiplier" term in $\delta^2 J^*$:

$$L(s) \equiv \mathbf{n}(s)^T(\mathbf{d_3})_{\theta\theta}(\theta(s)).$$

It will be convenient to write the term Z in a slightly different form. First, using the symmetry $\mathbf{M}(s,t) = \mathbf{M}(t,s)$, we can restrict the integration range of the outer two integrals from the unit square to the triangle $0 \le t \le s \le 1$, and double the result, canceling the leading factor of $1/2$:

$$Z = \int_0^1 \int_0^s \int_t^s \int_t^s h(\tau)h(\kappa)(\mathbf{d}_3)_\theta(\tau)^T\mathbf{M}(s,t)(\mathbf{d}_3)_\theta(\kappa)d\tau d\kappa dtds.$$

Now we reorder the integrals as $dt\ ds\ d\tau\ d\kappa$:

$$Z = \int_0^1 \int_0^1 \int_{\max(\tau,\kappa)}^1 \int_0^{\min(\tau,\kappa)} h(\tau)h(\kappa)(\mathbf{d}_3)_\theta(\tau)^T\mathbf{M}(s,t)(\mathbf{d}_3)_\theta(\kappa)dtds d\tau d\kappa.$$

We briefly justify the new limits of integration. First, the variables (τ,κ) can take on any values in the unit square, since any given values τ,κ are between t and s if $t = 0$ and $s = 1$. Then, for a given (τ,κ), the variable s can take on any value between $\max(\tau,\kappa)$ and 1 because we can, for example, have $t = 0$, and then both τ and κ will be between t and s, but s can not be below $\max(\tau,\kappa)$, since then either τ or κ (or both) will not be between s and any $t \le s$. Finally, for given values (τ,κ,s), the variable t can take on any value between 0 and $\min(\tau,\kappa)$ since then (τ,κ) will be between t and s, but t cannot be above $\min(\tau,\kappa)$ since then either τ or κ (or both) will not be between t and s. Thus,

$$Z = \frac{1}{2}\int_0^1 h(\tau)\left(\int_0^1 B(\kappa,\tau)h(\kappa)d\kappa\right)d\tau,$$

where

$$B(\kappa,\tau) \equiv 2(\mathbf{d}_3)_\theta(\theta(\tau))^T \left(\int_{\max(\tau,\kappa)}^1 \int_0^{\min(\tau,\kappa)} \mathbf{M}(s,t) dt ds \right) (\mathbf{d}_3)_\theta(\theta(\kappa)).$$

Combining the two pieces, the second variation becomes:

$$\delta^2 J^*[h] = \frac{1}{2} \int_0^1 h(\tau) \left[-Kh''(\tau) + L(\tau)h(\tau) + \int_0^1 B(\kappa,\tau)h(\kappa) d\kappa \right] d\tau,$$

where the integration variable s in the non-potential term has been renamed to τ, to combine with Z.

Thus, the second variation can be written as a quadratic form

$$\delta^2 J^*[h] = \frac{1}{2} \langle h, \mathcal{O}h \rangle,$$

where the operator $\mathcal{O}$ is defined by

$$\mathcal{O}h(\tau) \equiv \mathcal{S}h(\tau) + \mathcal{I}h(\tau), \tag{4.13}$$

where

$$\mathcal{S}h(\tau) \equiv -Kh''(\tau) + L(\tau)h(\tau)$$

is the differential piece (which would be the entire second-variation operator in the absence of the repulsive potential) and

$$\mathcal{I}h(\tau) \equiv \int_0^1 B(\kappa,\tau)h(\kappa) d\kappa$$

is the piece corresponding to the potential.

4.4. Determining the Index. In this section, we use the theory developed in Sec. 2 to compute an index for each critical point. We first embed the operator $\mathcal{O}$ in a particular family $\mathcal{O}_\sigma$ and establish a few properties of $\mathcal{O}_\sigma$, and also of its contact piece $\mathcal{I}_\sigma$. After introducing a projection operator to accommodate the integral constraint $\int_0^1 \sin\theta ds = 0$, we find the relevant definition of conjugate point for the planar rod problem as involving a projected variant of $\mathcal{O}_\sigma$, for which we address assumptions **A1** – **A4** using the properties of $\mathcal{O}_\sigma$ and $\mathcal{I}_\sigma$ proved earlier. We conclude by presenting algorithms for finding conjugate points and for determining the sign of the crossing velocity associated to each conjugate point.

4.4.1. Defining a family of eigenvalue problems. This problem has two additions to the classical theory sketched in Sec. 3: the contact potential term and the integral constraint. We will deal first with the contact potential term, by considering the family of Dirichlet spaces

$$C_d^2([0,\sigma]) \equiv \left\{ h \in C^2(0,\sigma) : h(0) = h(\sigma) = 0 \right\}$$

(these were the spaces $\tilde{\mathsf{A}}([0,\sigma])$ in Sec. 3, but here they are just an intermediate step), and the family of eigenvalue problems

$$\mathcal{O}_\sigma \boldsymbol{\zeta} = \rho(\sigma)\boldsymbol{\zeta} \text{ on } C_d^2([0,\sigma]) \tag{4.14}$$

for

$$\mathcal{O}_\sigma h(\tau) \equiv \mathcal{S}h(\tau) + \mathcal{I}_\sigma h(\tau), \tag{4.15}$$

where

$$\mathcal{I}_\sigma h(\tau) \equiv \int_0^\sigma B_\sigma(\kappa,\tau)h(\kappa)d\kappa,$$

for

$$B_\sigma(\kappa,\tau) \equiv 2(\mathbf{d}_3)_\theta(\theta(\tau))^T \left(\int_{\max(\tau,\kappa)}^{\sigma} \int_0^{\min(\tau,\kappa)} \mathbf{M}(s,t)dtds \right) (\mathbf{d}_3)_\theta(\theta(\kappa)).$$

In other words, the differential operator piece of $\mathcal{O}$ is left untouched, while the upper limits of the relevant integrals in the integral piece are changed from 1 to σ.

We will establish a few properties of the spectra for the family (4.14) of eigenvalue problems. First, by rescaling the independent variable, we can rewrite (4.14) so it involves a common space:

$$\overline{\mathcal{O}_\sigma}\boldsymbol{\zeta} = \rho(\sigma)\boldsymbol{\zeta} \text{ on } C_d^2([0,1])$$

for

$$\overline{\mathcal{O}_\sigma}h(\tau) = -\frac{1}{\sigma^2}h''(\tau) + \overline{\mathcal{W}_\sigma}h(\tau) + \overline{\mathcal{I}_\sigma}h(\tau),$$

where

$$\overline{\mathcal{I}_\sigma}h(\tau) \equiv \int_0^1 B_\sigma(\sigma\kappa,\sigma\tau)h(\kappa)d\kappa, \;\; \overline{\mathcal{W}_\sigma}h(\tau) \equiv L(\sigma\tau)h(\tau).$$

We define

$$\overline{\mathcal{V}_\sigma}h(\tau) \equiv -\frac{1}{\sigma^2}h''(\tau) + \overline{\mathcal{W}_\sigma}h(\tau)$$

4.4.2. Properties of $\overline{\mathcal{I}_\sigma}$ and $\overline{\mathcal{O}_\sigma}$. Since $\overline{\mathcal{O}_\sigma}$ is equal to the sum of the Sturm-Liouville operator $\overline{\mathcal{V}_\sigma}$ (which is known to obey these assumptions, as shown in Sec. 3) and the integral operator $\overline{\mathcal{I}_\sigma}$, we first establish some properties of $\overline{\mathcal{I}_\sigma}$.

LEMMA 4.2. *The operator $\overline{\mathcal{I}_\sigma} : L^2([0,1]) \to L^2([0,1])$ is symmetric.*

Proof. Defining the shorthand $\mathbf{\Pi}(s) \equiv (\mathbf{d}_3)_\theta(\theta(\sigma s))$, $\theta_m \equiv \min(\sigma\tau,\sigma\kappa)$ and $\theta_M \equiv \max(\sigma\tau,\sigma\kappa)$, we have

$$\langle h_1, \overline{\mathcal{I}_\sigma}h_2\rangle = 2\int_0^1\int_0^1\int_{\theta_M}^{\sigma}\int_0^{\theta_m} h_1(\tau)\mathbf{\Pi}(\tau)^T\mathbf{M}(s,t)\mathbf{\Pi}(\kappa)h_2(\kappa)dt\, ds\, d\kappa\, d\tau$$

The integrand is a scalar, so it is equal to its transpose:

$$\langle h_1, \overline{\mathcal{I}_\sigma}h_2\rangle = 2\int_0^1\int_0^1\int_{\theta_M}^{\sigma}\int_0^{\theta_m} h_2(\kappa)\mathbf{\Pi}(\kappa)^T\mathbf{M}(s,t)\mathbf{\Pi}(\tau)h_1(\tau)dt\, ds\, d\kappa\, d\tau$$

where we have used the fact that $\mathbf{M}$ is a symmetric matrix. Swapping the outer two integrals, and then renaming κ to τ and vice versa, we find:

$$\langle h_1, \overline{\mathcal{I}_\sigma}h_2\rangle = 2\int_0^1\int_0^1\int_{\theta_M}^{\sigma}\int_0^{\theta_m} h_2(\tau)\mathbf{\Pi}(\tau)^T\mathbf{M}(s,t)\mathbf{\Pi}(\kappa)h_1(\kappa)dt\, ds\, d\kappa\, d\tau = \langle h_2, \overline{\mathcal{I}_\sigma}h_1\rangle.$$

□

LEMMA 4.3. *The operator* $\overline{\mathcal{I}_\sigma} : L^2([0,1]) \to L^2([0,1])$ *is bounded with* $\|\overline{\mathcal{I}_\sigma}\| \leq 8\sigma^2\beta$.

Proof. First we recall that the mollifier included in the potential function f was chosen so that $\mathbf{M}(s,t) \to \mathbf{0}$ as $s \to t$. Therefore, $\mathbf{M}$ is continuous on the compact set $[0,1] \times [0,1]$, which means there will be a constant β so that each of the four entries of the matrix $\mathbf{M}(s,t)$ is less than or equal to β for all $s,t \in [0,1]$. Intuitively, the critical point $\mathbf{r}_0$ will have a "distance of closest approach" that minimizes $|\mathbf{r}(s) - \mathbf{r}(t)|$ for a pair of points on the rod where s, t are not close in arclength, say, $|s-t| > 0.1$ (see [13, Lemma 2] for an estimate of the distance of closest approach). Choosing $|\mathbf{x}|$ equal to this distance of closest approach provides an upper bound for the quantities $f_{\eta\eta}/|\mathbf{x}|^2$, $f_\eta/|\mathbf{x}|$, and $f_\eta/|\mathbf{x}|^3$ that comprise $\mathbf{M}$.

Since the entries of $(\mathbf{d}_3)_{\theta\theta}$ are bounded by 1 (they are either $\cos\theta$ or $\sin\theta$), we can see immediately that $|B_\sigma(\sigma\kappa, \sigma\tau)| \leq 8\sigma^2\beta$. Now,

$$\|\overline{\mathcal{I}_\sigma}h\|^2 = \int_0^1 \left| \int_0^1 B_\sigma(\sigma\kappa, \sigma\tau)h(\kappa)d\kappa \right|^2 d\tau \leq \int_0^1 \|B_\sigma(\cdot, \sigma\tau)\|^2 \|h\|^2 d\tau$$

by Hölder's Inequality. Since $|B_\sigma(\sigma\kappa, \sigma\tau)| \leq 8\sigma^2\beta$, we have:

$$\|\overline{\mathcal{I}_\sigma}h\|^2 \leq \int_0^1 \left(8\sigma^2\beta\|h\|\right)^2 d\tau = 64\sigma^4\beta^2\|h\|^2,$$

or $\|\overline{\mathcal{I}_\sigma}h\| \leq 8\sigma^2\beta\|h\|$, completing the proof. □

THEOREM 4.4. *The spectrum of* $\overline{\mathcal{O}_\sigma}$ *consists of a discrete set of eigenvalues* $\rho_1(\sigma) \leq \rho_2(\sigma) \leq \cdots$. *Furthermore, for* σ *sufficiently close to zero,* $\rho_1(\sigma) > 0$.

Proof. We know that $\overline{\mathcal{V}_\sigma}$ is a self-adjoint Sturm-Liouville operator obeying Legendre's strengthened condition, so its spectrum consists of a discrete set of isolated eigenvalues. The operator $\overline{\mathcal{O}_\sigma}$ is a perturbation of $\overline{\mathcal{V}_\sigma}$ by the bounded symmetric operator $\overline{\mathcal{I}_\sigma}$, and is therefore self-adjoint, and every element in the spectrum of $\overline{\mathcal{O}_\sigma}$ is within $\|\overline{\mathcal{I}_\sigma}\|$ of every element in the spectrum of $\overline{\mathcal{V}_\sigma}$ [14, p. 291]. Furthermore, since $\overline{\mathcal{I}_\sigma}$ is a compact operator [14, p. 157, Ex. 4.1] and the essential spectrum of $\overline{\mathcal{V}_\sigma}$ is empty, so must be the spectrum of $\overline{\mathcal{O}_\sigma}$ [1, p. 207]. Therefore, the spectrum of $\overline{\mathcal{O}_\sigma}$ must, like that of $\overline{\mathcal{V}_\sigma}$, be bounded below and have no accumulation points, and therefore consists of eigenvalues $\rho_1(\sigma) \leq \rho_2(\sigma) \leq \cdots$.

As noted in Sec. 3, we know by standard Sturm-Liouville theory that the eigenvalues of $\overline{\mathcal{V}_\sigma}$ are positive and bounded away from zero for $\sigma > 0$ small, i.e., there exists $\epsilon, \delta > 0$ so that $\rho_j(\sigma) > \epsilon$ for all $\sigma \in (0, \delta)$. That the same property holds for $\overline{\mathcal{O}_\sigma}$, which is $\overline{\mathcal{V}_\sigma}$ perturbed by $\overline{\mathcal{I}_\sigma}$, follows from a continuity argument as follows: the spectrum can change by at most $\|\overline{\mathcal{I}_\sigma}\|$ [14, p. 291], and by Lemma 4.3, $\|\overline{\mathcal{I}_\sigma}\| \leq 8\sigma^2\beta$, so therefore the eigenvalues of $\overline{\mathcal{O}_\sigma}$ are all positive for σ small (e.g., choose σ small enough that $8\sigma^2\beta < \epsilon$). □

4.4.3. Incorporating the integral constraint. Next we follow the methodology described in [17] to account for the presence of an isoperimetric constraint $\int_0^1 \sin(\theta(s))ds = 0$. As described above, the space of allowed variations is

$$\tilde{\mathsf{A}}([0,1]) = \{h \in C_d^2([0,1]) : \int_0^1 T(s)h(s)ds = 0\},$$

where

$$T(s) \equiv \cos(\theta(s)),$$

and for each $h \in \tilde{\mathsf{A}}([0,1])$, we have $\delta^2 J^*[h] = \frac{1}{2}\langle h, \mathcal{O}h\rangle$. (For the remainder of this section, we use this as the definition of $\tilde{\mathsf{A}}$ rather than the previous definition in Sec. 3.) However, to use the conjugate point theory outlined here, we may not use $\mathcal{O}$ as our second variation operator, because the range of $\mathcal{O}$ contains functions that are not in $\tilde{\mathsf{A}}([0,1])$ (since they do not satisfy the linearized integral constraint). To remedy this, we define $\mathcal{Q}$ to be the (self-adjoint) orthogonal projection that maps $L^2([0,1])$ onto the orthogonal complement within $L^2([0,1])$ of the function T. Since all $h \in \tilde{\mathsf{A}}([0,1])$ are orthogonal to T, we have $\mathcal{Q}h = h$, so that the second variation can be trivially rewritten as

$$\delta^2 J^*[h] = \frac{1}{2}\langle \mathcal{Q}h, \mathcal{O}\mathcal{Q}h\rangle = \frac{1}{2}\langle h, (\mathcal{Q}\mathcal{O}\mathcal{Q})\, h\rangle$$

Thus, we can take the operator $\mathcal{Q}\mathcal{O}\mathcal{Q}$ as our second variation operator, and if we define W to be the orthogonal complement of T in $L^2([0,1])$, then W contains the range of $\mathcal{Q}\mathcal{O}\mathcal{Q}$, and $\tilde{\mathsf{A}}([0,1])$ is dense in W, as required by our theory.

Next we need to embed the operator $\mathcal{Q}\mathcal{O}\mathcal{Q}$ and space $\tilde{\mathsf{A}}([0,1])$ within a σ-dependent family, and thus we define $\mathcal{Q}_\sigma$ to be the (self-adjoint) orthogonal projection that maps $L^2([0,\sigma])$ onto the orthogonal complement within $L^2([0,\sigma])$ of the function

$$T_\sigma(s) \equiv \cos(\theta(s/\sigma)).$$

Now we consider the operators $\mathcal{Q}_\sigma\mathcal{O}_\sigma\mathcal{Q}_\sigma$ and the eigenvalue problem $\mathcal{Q}_\sigma\mathcal{O}_\sigma\mathcal{Q}_\sigma h = \rho(\sigma)h$ on the family of spaces

$$\tilde{\mathsf{A}}([0,\sigma]) \equiv \{h \in C_d^2([0,\sigma]) : \int_0^\sigma h(s)T_\sigma(s)ds = 0\}$$

4.4.4. Assumptions A1 − A4. We will now address assumptions **A1-A4** for this family of eigenvalue problems, building on the properties proven above about the eigenvalue problem for $\mathcal{O}_\sigma$ on $C_d^2([0,\sigma])$. As discussed at the end of Sec. 2, we will not prove **A3** or the isolation of the eigenvalues in **A1**, since the perturbations of the Sturm-Liouville operator could, in principle, lead to the violation of these conditions, although not for a generic perturbation. We will address how such violations would be detected in the numerics (and no such evidence was seen).

First we note that our choice of $\mathcal{Q}_\sigma$ implies that if we rescale the independent variable to live on $[0,1]$ rather than $[0,\sigma]$, then we have the family of eigenvalue problems of the operator $\mathcal{Q}\overline{\mathcal{O}_\sigma}\mathcal{Q}$ on the common space $\tilde{\mathsf{A}}([0,1])$.

Since we showed in Thm. 4.4 that $\overline{\mathcal{O}_\sigma}$ has no essential spectrum on $C_d^2([0,1])$, the same follows for $\mathcal{Q}\overline{\mathcal{O}_\sigma}\mathcal{Q}$ on $\tilde{\mathsf{A}}([0,1])$ [17, p. 3067]. Thus the spectrum of $\mathcal{Q}\overline{\mathcal{O}_\sigma}\mathcal{Q}$ on $\tilde{\mathsf{A}}([0,1])$ consists of a discrete set of eigenvalues $\rho_1(\sigma) \le \rho_2(\sigma) \le \cdots$ (we know they are bounded below since the set of values of $\langle h, \mathcal{Q}\overline{\mathcal{O}_\sigma}\mathcal{Q}h\rangle$ for $h \in \tilde{\mathsf{A}}([0,1])$ is a subset of the set of the values of $\langle h, \overline{\mathcal{O}_\sigma}h\rangle$ for $h \in C_d^2([0,1])$. This verifies most of assumption **A1**, but not entirely, in that this argument can not show that the eigenvalues are simple. Indeed, for some $\overline{\mathcal{I}_\sigma}$, it may happen that some pair of isolated eigenvalues of the original operator $-(1/\sigma^2)(d^2/d\tau^2)$ may perturb to the same value in the spectrum of $\overline{\mathcal{O}_\sigma}$. We will assume that this does not happen in our application. For an arbitrarily chosen critical point, the probability of such a multiple eigenvalue

occurring should be zero. Furthermore, the existence of a non-simple eigenvalue would only really interfere with our index theory if it happened to a zero eigenvalue (an even more unlikely event), since that would cause us to miscount the number of eigenvalues changing sign at a conjugate point.

In a similar vein, we are not able to prove that assumption **A3** holds for our application. Recall that for the classic calculus of variations problem in Sec. 3, the eigenvalues ρ_i were decreasing functions of σ, and thus the same property holds for the eigenvalues of $\overline{\mathcal{V}_\sigma}$. However, upon perturbation by $\overline{\mathcal{I}_\sigma}$, the eigenvalues can in principle have turning points as σ varies, and thus the same might in principle be true for the projected operator $\mathcal{Q}\overline{\mathcal{O}_\sigma}\mathcal{Q}$. Indeed, this is an important realization that enables the extension of the classic conjugate point test to the more general index theory sketched in Sec. 2. We will assume that none of these turning points occurs at a zero eigenvalue. Again, among generic perturbations and choices of critical point, the existence of a turning point at a zero eigenvalue should be a probability-zero event.

Our numerical implementation should detect at least some of the non-generic violations of **A1** or **A3**, in ways that we outline in Sec. 4.4.5, and we saw no evidence of such violations.

Next, we verify assumption **A4**. Thm. 4.4 shows that, for σ sufficiently small, the lowest eigenvalue of $\overline{\mathcal{O}_\sigma}$ on $C^2_d([0,1])$ is positive. This implies that, for all $h \in C^2_d([0,1])$, we have $\langle h, \overline{\mathcal{O}_\sigma} h\rangle > 0$. Now let $h_1 \in \tilde{\mathsf{A}}([0,1]) \subset C^2_d([0,1])$ be the eigenvector of $\mathcal{Q}\overline{\mathcal{O}_\sigma}\mathcal{Q}$ corresponding to the smallest eigenvalue, i.e., $\mathcal{Q}\overline{\mathcal{O}_\sigma}\mathcal{Q}h_1 = \rho_1(\sigma)h_1$. Then, exploiting the fact that $\mathcal{Q}h_1 = h_1$,

$$\rho_1(\sigma) = \langle h_1, \mathcal{Q}\overline{\mathcal{O}_\sigma}\mathcal{Q}h_1\rangle = \langle \mathcal{Q}h_1, \overline{\mathcal{O}_\sigma}\mathcal{Q}h_1\rangle = \langle h_1, \overline{\mathcal{O}_\sigma}h_1\rangle > 0.$$

In preparation for verifying **A2**, we prove two lemmas relating to the continuity of the operators $\overline{\mathcal{I}_\sigma}$ and $\overline{\mathcal{W}_\sigma}$ with respect to σ.

LEMMA 4.5. *There exist constants γ, α so that for $0 \le \sigma \le \sigma^* \le 1$, we have*

$$\|\overline{\mathcal{W}_{\sigma^*}} - \overline{\mathcal{W}_\sigma}\| \le \gamma(\sigma^* - \sigma), \quad \|\overline{\mathcal{I}_{\sigma^*}} - \overline{\mathcal{I}_\sigma}\| \le \alpha(\sigma^* - \sigma).$$

Proof. The first claim follows easily from the fact that the function $L(s)$ is differentiable, hence Lipschitz. By definition, for any $h \in L^2([0,1])$,

$$\begin{aligned}
\left|\overline{\mathcal{I}_{\sigma^*}}h(\tau) - \overline{\mathcal{I}_\sigma}h(\tau)\right| &= \left|\int_0^1 \left[B_{\sigma^*}(\sigma^*\kappa, \sigma^*\tau) - B_\sigma(\sigma\kappa, \sigma\tau)\right] h(\kappa)d\kappa\right| \\
&\le \int_0^1 \left(|B_{\sigma^*}(\sigma^*\kappa, \sigma^*\tau) - B_{\sigma^*}(\sigma\kappa, \sigma\tau)| + |B_{\sigma^*}(\sigma\kappa, \sigma\tau) - B_\sigma(\sigma\kappa, \sigma\tau)|\right)|h(\kappa)|d\kappa \\
&\le \left(\int_0^1 \left(|B_{\sigma^*}(\sigma^*\kappa, \sigma^*\tau) - B_{\sigma^*}(\sigma\kappa, \sigma\tau)| + |B_{\sigma^*}(\sigma\kappa, \sigma\tau) - B_\sigma(\sigma\kappa, \sigma\tau)|\right)^2 d\kappa\right)^{1/2} \|h\|
\end{aligned}$$

(the last step is Hölder's Inequality). From the definition of B_σ, we have:

$$|B_{\sigma^*}(\sigma\kappa, \sigma\tau) - B_\sigma(\sigma\kappa, \sigma\tau)| = \left|2(\mathbf{d}_3)_\theta(\theta(\sigma\tau))^T \left(\int_\sigma^{\sigma^*} \int_0^{\min(\sigma\tau, \sigma\kappa)} \mathbf{M}(s,t)dtds\right)(\mathbf{d}_3)_\theta(\theta(\sigma\kappa))\right|.$$

Repeating the bounding argument used in the proof of Lemma 4.3, but adjusting for the fact that the rectangle of integration in the double integral above has area bounded by $\sigma^* - \sigma$, we find:

$$|B_{\sigma^*}(\sigma\kappa, \sigma\tau) - B_\sigma(\sigma\kappa, \sigma\tau)| \le 8\beta(\sigma^* - \sigma).$$

For the other term, we find Lipschitz bounds (uniform in σ) for $B_\sigma(\kappa,\tau)$ as a function of κ and τ (in $[0,\sigma]$). For example, for $\kappa<\tau$, we have

$$\frac{\partial B_\sigma}{\partial \kappa} = 2\left[(\mathbf{d_3})_\theta(\theta(\tau)\right]^T\left[\int_\tau^\sigma\int_0^\kappa \mathbf{M}(s,t)\,dt\,ds\right](\mathbf{d_3})_{\theta\theta}(\theta(\kappa))\theta'(\kappa)$$
$$+2\left[(\mathbf{d_3})_\theta(\theta(\tau)\right]^T\left[\int_\tau^\sigma \mathbf{M}(s,\kappa)ds\right](\mathbf{d_3})_\theta(\theta(\kappa)).$$

Since the entries of $\mathbf{M}$ are all between $-\beta$ and β, and the entries of $(\mathbf{d_3})_\theta$ and $(\mathbf{d_3})_{\theta\theta}$ are between -1 and 1, we have

$$\left|\frac{\partial B_\sigma}{\partial\kappa}\right| \le 8\beta\alpha_1 + 8\beta$$

where $\alpha_1 = \sup_{s\in[0,1]}|\theta'(s)|$. Therefore, for any $\kappa_1,\kappa_2\in[0,\tau]$, we have by the Mean Value Theorem that

$$|B_\sigma(\kappa_2,\tau) - B_\sigma(\kappa_1,\tau)| \le 8\beta(\alpha_1+1)|\kappa_2-\kappa_1|.$$

Repeating this argument for $\kappa>\tau$, we find the same Lipschitz bound for $\kappa_1,\kappa_2\in[\tau,1]$ (the partial derivative is different but has the same bound). Finally, if $\kappa_1<\tau<\kappa_2$, we have

$$\begin{aligned}|B_\sigma(\kappa_2,\tau) - B_\sigma(\kappa_1,\tau)| &\le |B_\sigma(\kappa_2,\tau) - B_\sigma(\tau,\tau)| + |B_\sigma(\tau,\tau) - B_\sigma(\kappa_1,\tau)|\\ &\le 8\beta(\alpha_1+1)(\kappa_2-\tau) + 8\beta(\alpha_1+1)(\tau-\kappa_1)\\ &= 8\beta(\alpha_1+1)(\kappa_2-\kappa_1).\end{aligned}$$

Thus $8\beta(\alpha_1+1)$ is a Lipschitz bound for B_σ as a function of κ (and an analogous argument gives the same Lipschitz bound for B_σ as a function of τ). Therefore,

$$|B_{\sigma^*}(\sigma^*\kappa,\sigma^*\tau) - B_{\sigma^*}(\sigma\kappa,\sigma\tau)| \le 8\beta(\alpha_1+1)(\sigma^*\kappa-\sigma\kappa) + 8\beta(\alpha_1+1)(\sigma^*\tau-\sigma\tau).$$

Therefore, combining the above results

$$\begin{aligned}\left|\overline{\mathcal{I}_{\sigma^*}}h(\tau) - \overline{\mathcal{I}_\sigma}h(\tau)\right| &\le \left(\int_0^1 \left(8\beta(\alpha_1+1)(\kappa+\tau)(\sigma^*-\sigma) + 8\beta(\sigma^*-\sigma)\right)^2 d\kappa\right)^{1/2}\|h\|\\ &= 8\beta(\sigma^*-\sigma)\left(\int_0^1\left((\alpha_1+1)(\kappa+\tau)+1\right)^2 d\kappa\right)^{1/2}\|h\|\\ &\le 8\beta(2\alpha_1+3)(\sigma^*-\sigma)\|h\|.\end{aligned}$$

Therefore, by the definition of operator norm, $\|\overline{\mathcal{I}_{\sigma^*}} - \overline{\mathcal{I}_\sigma}\| \le 8\beta(2\alpha_1+3)|\sigma^*-\sigma|$. □

Finally, we verify assumption **A2**, i.e., we prove that ρ_n is a continuous function of σ. Suppose not, i.e., ρ_n is not continuous at some particular σ. Then there exists $\epsilon>0$ and some sequence $\sigma_j\to\sigma$ such that $|\rho_n(\sigma_j)-\rho_n(\sigma)|>\epsilon$ for all j. In particular, one (or possibly both) of the following two cases must hold:

- Case I: there exists a sequence $\sigma_j\to\sigma$ such that $\rho_n(\sigma_j)>\rho_n(\sigma)+\epsilon$ for all j.
- Case II: there exists a sequence $\sigma_j\to\sigma$ such that $\rho_n(\sigma_j)<\rho_n(\sigma)-\epsilon$ for all j.

We will rule out each case and thereby complete the proof. We will use three fundamental properties of operators $\mathcal{M}$ with spectra of the type considered here:

(A) If x is a unit vector in the span of the first n eigenvectors of $\mathcal{M}$, then $\langle x, \mathcal{M}x\rangle$ is less than or equal to ρ_n, the nth smallest eigenvalue of $\mathcal{M}$.

(B) If X is an n-dimensional subspace of the domain of $\mathcal{M}$, then for some $x \in \mathsf{X}$, we have $\langle x, \mathcal{M}x\rangle \geq \rho_n$.

(C) If x is a unit vector orthogonal to the first $n-1$ eigenvectors of $\mathcal{M}$, then $\langle x, \mathcal{M}x\rangle \geq \rho_n$.

Property (A) follows by writing x as a linear combination of the first n eigenvectors, and (C) follows similarly by writing x as a linear combination of eigenvectors n and larger. Property (B) can be proven from the maximin characterization of eigenvalues (see (4.16) below).

Ruling out Case I

Let $h_1, \cdots h_n$ be unit eigenvectors corresponding to the smallest n eigenvalues of $\mathcal{Q}\overline{\mathcal{O}_\sigma}\mathcal{Q}$ on $\tilde{\mathsf{A}}([0,1])$, and let x be any unit vector in $\mathsf{B}_n \equiv \text{span}\{h_1, \cdots, h_n\}$, i.e., $x = c_1 h_1 + \cdots + c_n h_n$ where $(c_1)^2 + \cdots + (c_n)^2 = 1$. Then (integrating by parts)

$$\left|\left\langle x, -d^2x/ds^2\right\rangle\right| = |\langle x', x'\rangle| \leq \sum_{k=1}^{n}\sum_{l=1}^{n} |c_k c_l \langle h_k', h_l'\rangle| \leq n^2 \max_{k,l=1,\cdots,n} |\langle h_k', h_l'\rangle| .$$

Therefore, by Lemma 4.5,

$$\begin{aligned}
\left|\langle x, \mathcal{Q}\overline{\mathcal{O}_{\sigma_j}}\mathcal{Q}x\rangle - \langle x, \mathcal{Q}\overline{\mathcal{O}_\sigma}\mathcal{Q}x\rangle\right| &= \left|\langle x, \overline{\mathcal{O}_{\sigma_j}}x\rangle - \langle x, \overline{\mathcal{O}_\sigma}x\rangle\right| \\
&\leq \left|\frac{1}{(\sigma_j)^2} - \frac{1}{\sigma^2}\right| \left|\left\langle x, -\frac{d^2x}{ds^2}\right\rangle\right| \\
&\qquad + \left|\langle x, \left(\overline{\mathcal{I}_{\sigma_j}} + \overline{\mathcal{W}_{\sigma_j}} - \overline{\mathcal{I}_\sigma} - \overline{\mathcal{W}_\sigma}\right) x\rangle\right| \\
&\leq n^2 \max_{k,l=1,\cdots,n} |\langle h_k', h_l'\rangle| \left|\frac{1}{(\sigma_j)^2} - \frac{1}{\sigma^2}\right| + (\alpha+\gamma)|\sigma_j - \sigma|.
\end{aligned}$$

Therefore, since $\sigma_j \to \sigma$, and the above bound goes to zero in that limit, we have some natural number J so that for $j \geq J$ and all $x \in \mathsf{B}_n$,

$$\langle x, \mathcal{Q}\overline{\mathcal{O}_{\sigma_j}}\mathcal{Q}x\rangle < \langle x, \mathcal{Q}\overline{\mathcal{O}_\sigma}\mathcal{Q}x\rangle + \epsilon.$$

By property (A), $\langle x, \mathcal{Q}\overline{\mathcal{O}_\sigma}\mathcal{Q}x\rangle \leq \rho_n(\sigma)$, and by property (B), for some $x \in \mathsf{B}_n$, we have $\langle x, \mathcal{Q}\overline{\mathcal{O}_{\sigma_j}}\mathcal{Q}x\rangle \geq \rho_n(\sigma_j)$. Combining these facts with the inequality above, we find that $\rho_n(\sigma_j) < \rho_n(\sigma) + \epsilon$ for $j \geq J$, which contradicts Case I.

Ruling out Case II

On the other hand, suppose that Case II holds. By the maximin characterization of $\rho_n(\sigma_j)$ [29, p. 24], we have

$$\rho_n(\sigma_j) = \max_{p_1,\cdots,p_{n-1}} \min_x \langle x, \mathcal{Q}\overline{\mathcal{O}_{\sigma_j}}\mathcal{Q}x\rangle \tag{4.16}$$

where $\{p_1, \cdots, p_{n-1}\}$ ranges over all orthonormal sets in $\tilde{\mathsf{A}}([0,1])$ and x ranges over all unit vectors in $\tilde{\mathsf{A}}([0,1])$ orthonormal to all the vectors p_j. Thus, since Case II says that $\rho_n(\sigma_j) < \rho_n(\sigma) - \epsilon$ for all j, it must be that for any choice of orthonormal set $\{p_1, \cdots, p_{n-1}\}$, we have, for all j,

$$\min_x \langle x, \mathcal{Q}\overline{\mathcal{O}_{\sigma_j}}\mathcal{Q}x\rangle < \rho_n(\sigma) - \epsilon.$$

In particular, if we choose $p_j = h_j$, there exists some unit vector x orthogonal to all of the first $n-1$ eigenvectors of $\mathcal{Q}\overline{\mathcal{O}_\sigma}\mathcal{Q}$ so that

$$\langle x, \mathcal{Q}\overline{\mathcal{O}_{\sigma_j}}\mathcal{Q}x\rangle < \rho_n(\sigma) - \epsilon. \tag{4.17}$$

Now, for this vector x, we have:

$$\begin{aligned}\left|\langle x, \mathcal{Q}\overline{\mathcal{O}_{\sigma_j}}\mathcal{Q}x\rangle - \langle x, \mathcal{Q}\overline{\mathcal{O}_\sigma}\mathcal{Q}x\rangle\right| &= \left|\langle x, \overline{\mathcal{O}_{\sigma_j}}x\rangle - \langle x, \overline{\mathcal{O}_\sigma}x\rangle\right| \\ &\le \left|\frac{1}{(\sigma_j)^2} - \frac{1}{\sigma^2}\right| \left|\left\langle x, -\frac{d^2x}{ds^2}\right\rangle\right| \\ &\quad + \left|\langle x, \left(\overline{\mathcal{I}_{\sigma_j}} + \overline{\mathcal{W}_{\sigma_j}} - \overline{\mathcal{I}_\sigma} - \overline{\mathcal{W}_\sigma}\right)x\rangle\right| \\ &\le \left|\left\langle x, -\frac{d^2x}{ds^2}\right\rangle\right| \left|\frac{1}{(\sigma_j)^2} - \frac{1}{\sigma^2}\right| + (\alpha+\gamma)|\sigma_j - \sigma|.\end{aligned}$$

Therefore, since $\sigma_j \to \sigma$, and the above bound goes to zero in that limit, we have some natural number J so that for $j \ge J$,

$$\langle x, \mathcal{Q}\overline{\mathcal{O}_{\sigma_j}}\mathcal{Q}x\rangle > \langle x, \mathcal{Q}\overline{\mathcal{O}_\sigma}\mathcal{Q}x\rangle - \epsilon.$$

But by property (C), $\langle x, \mathcal{Q}\overline{\mathcal{O}_\sigma}\mathcal{Q}x\rangle \ge \rho_n(\sigma)$, so we have shown that for $j \ge J$,

$$\langle x, \mathcal{Q}\overline{\mathcal{O}_{\sigma_j}}\mathcal{Q}x\rangle > \rho_n(\sigma) - \epsilon, \tag{4.18}$$

which contradicts the inequality (4.17). Thus, Case II is not possible.

4.4.5. Algorithm for finding conjugate points. The previous section developed the theoretical basis for using conjugate points as a means of determining the index of a critical point. In this section, we discuss how to numerically compute the number of conjugate points corresponding to each solution. Consider nontrivial solutions to the conjugate point equation

$$\mathcal{Q}_\sigma\mathcal{O}_\sigma\mathcal{Q}_\sigma h = 0, \quad h(0) = h(\sigma) = 0, \quad \langle h, T_\sigma\rangle = 0, \tag{4.19}$$

where $\langle\ ,\ \rangle$ is the L^2 inner product on $[0,\sigma]$. Since h is required to be orthogonal to T_σ on $[0,\sigma]$, we have $\mathcal{Q}_\sigma h = h$. Also, since $\mathcal{Q}_\sigma$ is the projection onto the orthogonal complement of T_σ, the definition of projection allows (4.19) to be written in the form

$$(\mathcal{S}h)(\tau) + \int_0^\sigma B_\sigma(\kappa,\tau)h(\kappa)d\kappa = cT_\sigma(\tau), \quad h(0) = h(\sigma) = 0, \quad \langle h, T_\sigma\rangle = 0, \tag{4.20}$$

where c is any real number. To solve (4.20), we will solve both the homogeneous system:

$$(\mathcal{S}h)(\tau) + \int_0^\sigma B_\sigma(\kappa,\tau)h(\kappa)d\kappa = 0, \quad h(0) = 0, \quad h'(0) = 1 \tag{4.21}$$

(call this solution h^{hom}), and the nonhomogeneous system:

$$(\mathcal{S}h)(\tau) + \int_0^\sigma B_\sigma(\kappa,\tau)h(\kappa)d\kappa = T_\sigma(\tau), \quad h(0) = 0, \quad h'(0) = 0 \tag{4.22}$$

(call this solution h^{non}). Then any solution h to (4.20) without the conditions $h(\sigma) = 0$ and $\langle h, T_\sigma\rangle = 0$ is a linear combination $\check{c}h^{hom} + ch^{non}$ where c is the constant from

(4.20) and $\breve{c} = h'(0)$. Then, the two conditions $h(\sigma) = 0$ and $\langle h, T_\sigma \rangle = 0$ are enforced by solving the linear system

$$\begin{bmatrix} h^{hom}(\sigma) & h^{non}(\sigma) \\ \langle h^{hom}, T_\sigma \rangle & \langle h^{non}, T_\sigma \rangle \end{bmatrix} \begin{bmatrix} \breve{c} \\ c \end{bmatrix} = \mathbf{0}, \tag{4.23}$$

which means that the 2×2 matrix must have determinant zero.

To numerically determine h^{hom} and h^{non} given a numerical approximation to a critical point $(\theta, \mathbf{n}, \mathbf{r})$ computed on a uniform grid of $[0, 1]$ with N subintervals, we do the following. We run a loop of $\sigma = k/N$ for $k = 4$ through N. For each k, we determine a numerical approximation to h^{hom} by discretizing (4.21) at $k - 1$ interior points of $[0, k/N]$, to find the unknowns $h_2 = h^{hom}(2/N)$ through $h_k = h^{hom}(k/N)$, with $h^{hom}(0) = 0$ and $h^{hom}(1/N) \approx (h^{hom})'(0)/N = 1/N$ known from the boundary conditions. The expression $\mathcal{S}h = -Kh'' + [(\mathbf{n})^T(\mathbf{d_3})_{\theta\theta}(\theta)]h$ is discretized via a standard central difference. The integral $\int_0^{k/N} B_\sigma(\kappa, \tau)h(\kappa)\, d\kappa$ is discretized via the trapezoid rule. This discretization of (4.21) yields $k - 1$ linear equations for the $k-1$ unknowns $h_2, \cdots, h_k$, and the last unknown is our computed value for the upper left entry in the "stability matrix" in (4.23). The lower-left entry of this matrix is computed by applying the trapezoid rule using the computed values $h_2, \cdots, h_k$ (and the known values h_0 and h_1).

A similar procedure applied to (4.22) allows us to compute the upper right and lower right entries of the stability matrix.

As k advances through the loop, whenever the determinant of the stability matrix crosses zero, we have a conjugate point. We estimate the exact location σ of the conjugate point via the secant method, and then compute the velocity of the zero eigenvalue as described in the next section.

We pause to consider how violations of **A3** or the simple eigenvalue portion of **A1** would be manifested in this numerical implementation. If two more more eigenvalues pass through zero at the same instant, then we should see numerical instability in solving (4.21) or (4.22) (if either of these equations individually does not yield a unique solution), or the matrix in (4.23) should become rank-zero (if more than one combination of the solutions to (4.21) and (4.22) yields a conjugate point). If an eigenvalue has a turning point at zero, then the computed velocity of the zero eigenvalue should be close to zero. We saw none of these effects in our computations.

Especially with critical points for which contact is considerable, the determinant of the stability matrix can become rapidly oscillatory close to $\sigma = 1$, which can make it more difficult to detect zero crossings.[2] This can be addressed by increasing N or (more efficiently) by locally refining the grid of σ values where the stability matrix is computed. The determinant of the stability matrix appears to obey the Sturm separation theorem (zeroes of the determinant and its derivative alternate), so we have found that refining the grid at apparent turning points in the determinant that would violate the separation theorem is a successful strategy in finding all of the conjugate points.

Some precomputation (before the σ loop has begun) allows for a more efficient determination of the values of $B_\sigma(\kappa, \tau)$. First, we compute numerical estimates for

[2]We note that this rapid oscillation appears to be alleviated if we require h to be orthogonal to the restriction of T to $[0, \sigma]$ rather than to T_σ. This alternate choice for embedding the $\sigma = 1$ eigenvalue problem within a family may thus be preferable numerically. We have chosen the T_σ embedding here because it seems to facilitate the verification of **A2** (since we can rescale so that all the eigenvalue problems occur on a common space) but we see no reason to doubt that **A2** also holds for the other choice.

all values of

$$C_1(s,\chi) \equiv 2\int_0^{\chi} \mathbf{M}(s,t)dt$$

for $0 < \chi \leq s \leq 1$ with χ, s multiples of $1/N$, and then use those to precompute numerical estimates for all values of

$$C_2(\psi,\chi) \equiv \int_{\psi}^{1} C_1(s,\chi)\, ds$$

for $0 < \chi \leq \psi \leq 1$ with χ, ψ multiples of $1/N$. Then, for any σ that is a multiple of $1/N$, and for any i, j with $i/N, j/N \leq \sigma$, the quantity $B_\sigma(j/N, i/N)$ can be determined quickly via the formula

$$B_\sigma\left(\frac{j}{N}, \frac{i}{N}\right) = (\mathbf{d_3})_\theta\left(\theta\left(\frac{i}{N}\right)\right)^T \left[C_2\left(\frac{\max(i,j)}{N}, \frac{\min(i,j)}{N}\right) - C_2\left(\sigma, \frac{\min(i,j)}{N}\right)\right](\mathbf{d_3})_\theta\left(\theta\left(\frac{j}{N}\right)\right). \tag{4.24}$$

4.4.6. Crossing Velocity. Assume that there is a conjugate point, that is, a value of σ such that $\rho(\sigma) = 0$. Since we assume that the crossing is transverse (assumption **A3**), in a neighborhood of σ, ths eigenvalue will cross zero with either a negative velocity or a positive velocity. Here we derive (via a perturbation argument) a computation for determining the sign of this "crossing velocity".

For each $s \in (0,1)$, we let $\rho_j(s)$ be the eigenvalues of $\mathcal{Q}_s\mathcal{O}_s\mathcal{Q}_s$, with corresponding normalized eigenfunction denoted as $h_j(\cdot; s)$. We assume that σ is a conjugate point, so that $\rho_j(\sigma) = 0$ for some j. We seek to determine the sign of $\rho_j(\sigma - \epsilon)$ for some small $\epsilon > 0$: if $\rho_j(\sigma - \epsilon) < 0$, the conjugate point has positive-velocity; otherwise it has negative-velocity.

We first note that, by the construction of T_σ, the function

$$\chi(s) \equiv h_j\left(\frac{\sigma s}{\sigma - \epsilon}; \sigma\right)$$

is an element of the domain $\tilde{\mathsf{A}}([0, \sigma - \epsilon])$, since it vanishes at $s = 0$ and $s = \sigma - \epsilon$ and is orthogonal on $[0, \sigma - \epsilon]$ to $T_{\sigma-\epsilon}$ (as can be seen by rescaling s by $\sigma - \epsilon$).

Claim: For ϵ sufficiently small, the sign of $\langle \chi, \mathcal{O}_{\sigma-\epsilon}\chi\rangle$ (with the inner product on $[0, \sigma - \epsilon]$) is the same as the sign of $\rho_j(\sigma - \epsilon)$.

Proof.

Let $\hat{\chi}$ be the $L^2([0, \sigma - \epsilon])$-normalized scaling of χ; clearly the sign of $\langle \hat{\chi}, \mathcal{O}_{\sigma-\epsilon}\hat{\chi}\rangle$ is the same as the sign of $\langle \chi, \mathcal{O}_{\sigma-\epsilon}\chi\rangle$. Then, if we assume that the eigenfunctions, like the eigenvalues, are continuous in σ, we must have

$$\hat{\chi}(s) = \sqrt{1 - b^2}\, h_j(s; \sigma - \epsilon) + b h_r(s),$$

where $b = O(\epsilon)$ and h_r is a unit vector orthogonal to $h_j(\cdot; \sigma - \epsilon)$. Expanding h_r in the remaining eigenfunctions at $\sigma - \epsilon$:

$$\hat{\chi}(s) = \sqrt{1 - b^2}\, h_j(s; \sigma - \epsilon) + b\sum_{i \neq j} c_i h_i(s; \sigma - \epsilon).$$

Next we note that since $\langle \hat{\chi}, T_{\sigma-\epsilon}\rangle = 0$ on $[0, \sigma-\epsilon]$, we have $\mathcal{Q}_{\sigma-\epsilon}\hat{\chi} = \hat{\chi}$, so that

$$\langle \hat{\chi}, \mathcal{O}_{\sigma-\epsilon}\hat{\chi}\rangle = \langle \hat{\chi}, \mathcal{Q}_{\sigma-\epsilon}\mathcal{O}_{\sigma-\epsilon}\mathcal{Q}_{\sigma-\epsilon}\hat{\chi}\rangle.$$

Then, since the h_i are orthonormal eigenfunctions of $\mathcal{Q}_{\sigma-\epsilon}\mathcal{O}_{\sigma-\epsilon}\mathcal{Q}_{\sigma-\epsilon}$, a straightforward computation shows that:

$$\langle \hat{\chi}, \mathcal{O}_{\sigma-\epsilon}\hat{\chi}\rangle = (1-b^2)\rho_j(\sigma-\epsilon) + b^2\sum_{i\neq j}(c_i)^2\rho_i(\sigma-\epsilon).$$

Since $b = O(\epsilon)$ and $\rho_j(\sigma-\epsilon) = O(\epsilon)$, the first term dominates the second term, so that

$$\langle \hat{\chi}, \mathcal{O}_{\sigma-\epsilon}\hat{\chi}\rangle = \rho_j(\sigma-\epsilon) + O(\epsilon^2).$$

Since $\rho_j(\sigma-\epsilon) = O(\epsilon)$, we can see that for ϵ sufficiently small, $\rho_j(\sigma-\epsilon)$ has the same sign as $\langle \hat{\chi}, \mathcal{O}_{\sigma-\epsilon}\hat{\chi}\rangle$, and hence the same sign as $\langle \chi, \mathcal{O}_{\sigma-\epsilon}\chi\rangle$.
□

Finally, we derive an expression that is independent of ϵ and has the same sign as the small-ϵ limit of $\langle \chi, \mathcal{O}_{\sigma-\epsilon}\chi\rangle$, and that furthermore is convenient to compute given the computational scheme described in the previous section. We have

$$\langle \chi, \mathcal{O}_{\sigma-\epsilon}\chi\rangle = \int_0^{\sigma-\epsilon} h_j\left(\frac{\sigma s}{\sigma-\epsilon};\sigma\right)\left[-\frac{K\sigma^2}{(\sigma-\epsilon)^2}h_j''\left(\frac{\sigma s}{\sigma-\epsilon};\sigma\right) + L(s)h_j\left(\frac{\sigma s}{\sigma-\epsilon};\sigma\right) + \int_0^{\sigma-\epsilon} B_{\sigma-\epsilon}(\kappa, s)h_j\left(\frac{\sigma\kappa}{\sigma-\epsilon};\sigma\right)d\kappa\right]ds.$$

The change of variables $\tau \equiv \sigma s/(\sigma-\epsilon)$ in the outer integral yields:

$$\langle \chi, \mathcal{O}_{\sigma-\epsilon}\chi\rangle = \frac{\sigma-\epsilon}{\sigma}\int_0^{\sigma} h_j(\tau;\sigma)\left[-\frac{K\sigma^2}{(\sigma-\epsilon)^2}h_j''(\tau;\sigma) + L\left(\frac{(\sigma-\epsilon)\tau}{\sigma}\right)h_j(\tau;\sigma) + \int_0^{\sigma-\epsilon} B_{\sigma-\epsilon}\left(\kappa, \frac{(\sigma-\epsilon)\tau}{\sigma}\right)h_j\left(\frac{\sigma\kappa}{\sigma-\epsilon};\sigma\right)d\kappa\right]d\tau.$$

Since we are only concerned with the sign of $\langle \chi, \mathcal{O}_{\sigma-\epsilon}\chi\rangle$, we will henceforth consider

$$E \equiv \int_0^{\sigma} h_j(\tau;\sigma)\left[-\frac{K\sigma^2}{(\sigma-\epsilon)^2}h_j''(\tau;\sigma) + L\left(\frac{(\sigma-\epsilon)\tau}{\sigma}\right)h_j(\tau;\sigma) + \int_0^{\sigma-\epsilon} B_{\sigma-\epsilon}\left(\kappa, \frac{(\sigma-\epsilon)\tau}{\sigma}\right)h_j\left(\frac{\sigma\kappa}{\sigma-\epsilon};\sigma\right)d\kappa\right]d\tau.$$

Now, we note that since $0 = \rho_j(\sigma) = \langle h_j(\cdot;\sigma), \mathcal{O}_\sigma h_j(\cdot;\sigma)\rangle$, we have

$$0 = \int_0^{\sigma} h_j(\tau;\sigma)\left[-Kh_j''(\tau;\sigma) + L(\tau)h_j(\tau;\sigma) + \int_0^{\sigma} B_\sigma(\kappa,\tau)h_j(\kappa;\sigma)d\kappa\right]d\tau.$$

Thus,

$$E = \int_0^{\sigma}\left[L\left(\frac{(\sigma-\epsilon)\tau}{\sigma}\right) - \frac{\sigma^2}{(\sigma-\epsilon)^2}L(\tau)\right](h_j(\tau;\sigma))^2\,d\tau + \int_0^{\sigma}\int_0^{\sigma-\epsilon} B_{\sigma-\epsilon}\left(\kappa, \frac{(\sigma-\epsilon)\tau}{\sigma}\right)h_j(\tau;\sigma)h_j\left(\frac{\sigma\kappa}{\sigma-\epsilon};\sigma\right)d\kappa d\tau - \int_0^{\sigma}\int_0^{\sigma}\frac{\sigma^2}{(\sigma-\epsilon)^2}B_\sigma(\kappa,\tau)h_j(\tau;\sigma)h_j(\kappa;\sigma)d\kappa d\tau.$$

By Taylor expansion,

$$L\left(\frac{(\sigma-\epsilon)\tau}{\sigma}\right) - \frac{\sigma^2}{(\sigma-\epsilon)^2}L(\tau) = -\frac{\epsilon\tau}{\sigma}L'(\tau) - \frac{2\epsilon}{\sigma}L(\tau) + O(\epsilon^2)$$

In the first double integral, we change variables from κ to $\sigma\kappa/(\sigma-\epsilon)$ (but still calling it κ for convenient comparison to the second double integral) to find

$$\frac{\sigma-\epsilon}{\sigma}\int_0^\sigma\int_0^\sigma B_{\sigma-\epsilon}\left(\frac{(\sigma-\epsilon)\kappa}{\sigma},\frac{(\sigma-\epsilon)\tau}{\sigma}\right)h_j(\tau;\sigma)h_j(\kappa;\sigma)d\kappa d\tau.$$

Now, if we expand the two double integrals in ϵ, the $O(1)$ terms will cancel, so we merely compute the $O(\epsilon)$ terms. For the first double integral, this $O(\epsilon)$ term is

$$\begin{aligned}&-\frac{\epsilon}{\sigma}\int_0^\sigma\int_0^\sigma B_\sigma(\kappa,\tau)h_j(\tau;\sigma)h_j(\kappa;\sigma)d\kappa d\tau - \epsilon\int_0^\sigma\int_0^\sigma\frac{\partial B_\sigma}{\partial\sigma}(\kappa,\tau)h_j(\tau;\sigma)h_j(\kappa;\sigma)d\kappa\,d\tau\\ &-\frac{\epsilon}{\sigma}\int_0^\sigma\int_0^\sigma\rho\frac{\partial B_\sigma}{\partial\kappa}(\kappa,\tau)h_j(\tau;\sigma)h_j(\kappa;\sigma)d\kappa\,d\tau - \frac{\epsilon}{\sigma}\int_0^\sigma\int_0^\sigma\tau\frac{\partial B_\sigma}{\partial\tau}(\kappa,\tau)h_j(\tau;\sigma)h_j(\kappa;\sigma)d\kappa\,d\tau,\end{aligned} \tag{4.25}$$

while for the second double integral, the $O(\epsilon)$ term is

$$-\frac{2\epsilon}{\sigma}\int_0^\sigma\int_0^\sigma B_\sigma(\kappa,\tau)h_j(\tau;\sigma)h_j(\kappa;\sigma)d\kappa d\tau.$$

Adding these together (and noting that the third and fourth integrals in (4.25) are equal, since $B_\sigma(\kappa,\tau) = B_\sigma(\tau,\kappa)$ for all τ,κ), we have:

$$\begin{aligned}E = -\epsilon\Bigg(&\int_0^\sigma\left[\frac{\tau}{\sigma}L'(\tau)+\frac{2}{\sigma}L(\tau)\right](h_j(\tau;\sigma))^2\,d\tau\\ &+\int_0^\sigma\int_0^\sigma\left[\frac{3}{\sigma}B_\sigma(\kappa,\tau)+\frac{\partial B_\sigma}{\partial\sigma}(\kappa,\tau)+\frac{2\kappa}{\sigma}\frac{\partial B_\sigma}{\partial\kappa}(\kappa,\tau)\right]h_j(\tau;\sigma)h_j(\kappa;\sigma)d\kappa d\tau\Bigg)+O(\epsilon^2).\end{aligned}$$

Thus, in order to compute $\langle\chi,\mathcal{O}_{\sigma-\epsilon}\chi\rangle$ correct to leading order in ϵ, we numerically compute (via the trapezoid rule) the following integrals:

$$\begin{aligned}&\int_0^\sigma L(\tau)\left(h_j(\tau;\sigma)\right)^2 d\tau,\quad \int_0^\sigma \tau L'(\tau)\left(h_j(\tau;\sigma)\right)^2 d\tau,\quad \int_0^\sigma\int_0^\sigma B_\sigma(\kappa,\tau)h_j(\kappa;\sigma)h_j(\tau;\sigma)d\kappa d\tau,\\ &\int_0^\sigma\int_0^\sigma\frac{\partial B_\sigma}{\partial\sigma}(\kappa,\tau)h_j(\kappa;\sigma)h_j(\tau;\sigma)d\kappa d\tau,\quad \int_0^\sigma\int_0^\sigma\kappa\frac{\partial B_\sigma}{\partial\kappa}(\kappa,\tau)h_j(\kappa;\sigma)h_j(\tau;\sigma)d\kappa d\tau,\end{aligned}$$

taking advantage of (4.24) to efficiently compute B_σ. Single-integral expressions for $\partial B_\sigma/\partial\sigma$ and $\partial B_\sigma/\partial\kappa$ can be computed from the definition of B_σ, and these single integrals can be derived from the pre-computed values of C_1 from Sec. 4.4.5 via a formula analogous to (4.24). Similarly, it is straightforward to write down L' in terms of θ, $\mathbf{n}$, θ', and $\mathbf{n}'$ (the latter two of which we estimate by finite difference).

4.5. Results. Using the methods described in the previous sections, families of critical points were computed and an index assigned to each critical point. The results are shown in Figs. 4.3, 4.4, and 4.5.

Each figure shows a bifurcation diagram of the loading force λ plotted against the height $z(1)$, with the solid lines corresponding to solutions for a given value

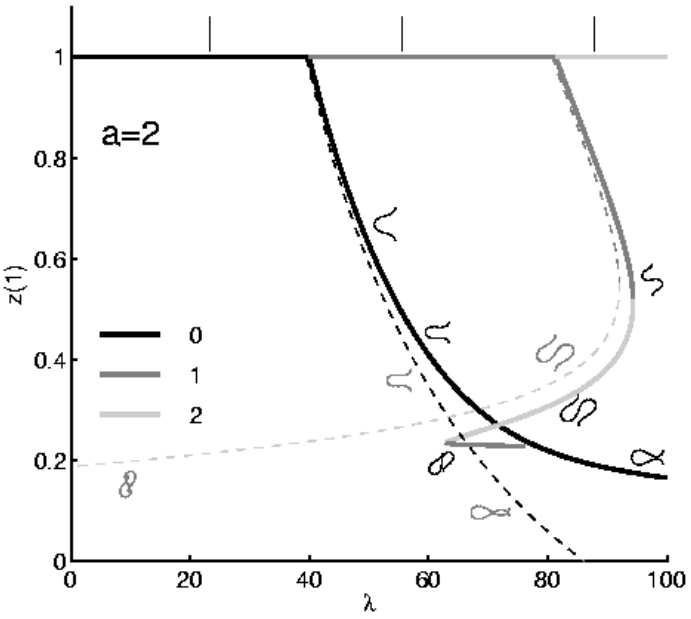

FIG. 4.3. *The bifurcation diagram of the planar elastic rod with repulsive force strength $a = 2$ (with $a = 0$ shown as a dashed line), plotting loading force λ and the rod height $z(1)$ for a variety of critical points. Some sample configurations are shown as insets. The index is indicated by grayscale. The horizontal line at $z(1) = 1$ consists of straight configurations with varying amounts of loads. Branches of buckled solutions emerge from this branch at a sequence of bifurcation points.*

of the repulsive force strength parameter a and the dashed lines for "non-contact" solutions with $a = 0$ (so that the rod is allowed to pass through itself with no penalty). Representative shapes of the rod are shown as insets in Fig. 4.3. The index is depicted by grayscale, as illustrated in the figure legends.

Each diagram contains a branch of straight-rod solutions (the horizontal line at $z(1) = 1$), and two curves of buckled-rod solutions branching off at bifurcation points. (There are an infinite number of such branches, but only the first two are shown.) Each branch was computed by a three-stage parameter continuation. We start at a value of λ somewhat before the bifurcation point in question, with an intrinsic shape $\hat{\theta}(s) = \beta s^4/12$ (the particular formula is not important) for a small value of $\beta > 0$, and use the straight rod as the initial guess for the solution of the equilibrium equations (4.9). The first stage of parameter continuation increases λ somewhat past the bifurcation value, and, because of the presence of intrinsic shape, the computed solutions track closely the desired bifurcating branch (if we had $\beta = 0$, we would just stay on the branch of straight-rod solutions as λ increased). The second stage decreases β to zero, turning off the intrinsic shape. The third stage decreases λ, so that we backtrack to the bifurcation point and then "bounce" off it and compute the entire branch of buckled solutions. (In truth, the bifurcation point is a pitchfork, the two outer tines of which lie on top of each other in our chosen $(\lambda, z(1))$ diagram, so we are not really bouncing but rather moving smoothly to the other half of the pitchfork.)

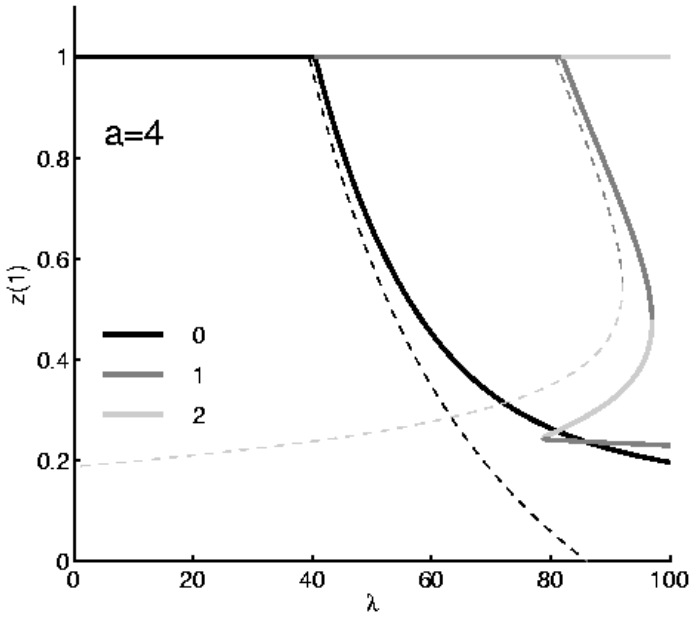

FIG. 4.4. *The bifurcation diagram of the planar elastic rod with repulsive force strength $a = 4$ (with $a = 0$ shown as a dashed line), plotting loading force λ and the rod height $z(1)$ for a variety of critical points.*

As one would expect from classical theory, the straight-rod solution is stable (has index zero) to the first bifurcation point, then unstable, with the index increasing by one at each bifurcation point.

The first bifurcating branch closely tracks the corresponding $a = 0$ branch, but diverges from it for larger values of λ, with the divergence more pronounced for larger values of a (since larger forces are required to counteract the larger repulsive force). For both the contact and non-contact problems, this branch contains stable solutions. (Actually, the non-contact branch dips below $z(1) = 0$ outside the region we have graphed, and these configurations are unstable, with index one. The contact branch does not cross $z(1) = 0$ since the repulsive force prevents the rod from passing through itself.)

The second bifurcating branch begins with index-one solutions for both the contact and non-contact problems. For small values of a (and for $a = 0$), this branch folds and becomes index-two. Further on this branch, the repulsive force has a stabilizing influence, causing a second fold that returns the index to one (while the non-contact problem remains at index two). For $a = 8$, the repulsive force eliminates the first fold altogether, so that the branch stays at index one.

These results can be partially verified using the independent idea of distinguished diagrams, which predicts the change in index at a fold in the appropropiate bifurcation diagram. In the next section, we verify that the $(\lambda, z(1))$ diagram is "distinguished", and that the change in index seen in the folds in Figs. 4.3 and 4.4 match this theory.

5. Distinguished Diagrams. A complementary method for determining stability is that of distinguished bifurcation diagrams, pioneered by Thompson [25] in

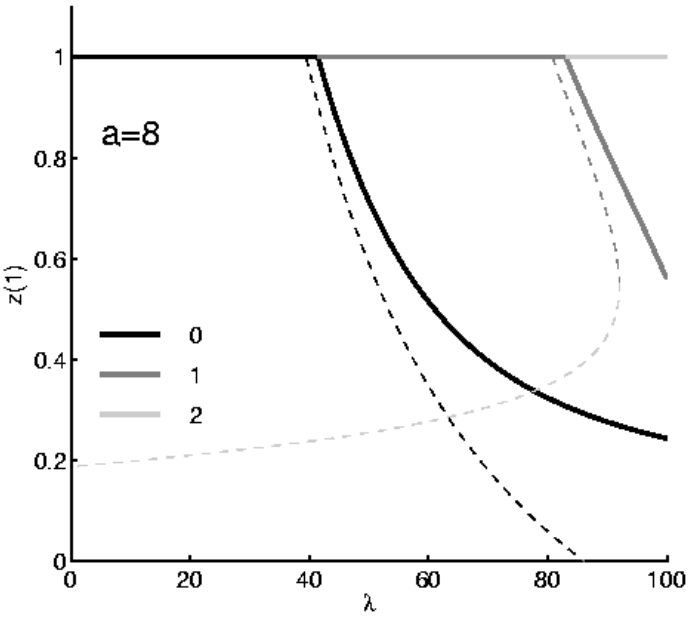

FIG. 4.5. *The bifurcation diagram of the planar elastic rod with repulsive force strength $a = 2$ (with $a = 0$ shown as a dashed line), plotting loading force λ and the rod height $z(1)$ for a variety of critical points.*

finite dimensions, and by Maddocks [16] for calculus of variations problems. The essential idea of distinguished diagrams is that certain projections of a bifurcation diagram allow one to determine how stability changes at a fold. Typically, the ordinate of the distinguished diagram gives information regarding the sign of the derivative of a specific eigenvalue that is zero at the fold, which, for example, indicates which branch of the fold has a negative eigenvalue and hence does not correspond to minima of the functional.

Previously, distinguished diagrams have been determined in several problems involving the classic functional from Sec. 3, for problems with or without isoperimetric constraints, and where the bifurcation parameter appears in the functional, in the boundary conditions, or as a Lagrange multiplier [16, 12]. For the planar rod example in Sec. 4, the distinguishing feature is the repulsion term that appears in the functional. The following calculation shows that the distinguished diagram results that appeared in [16] and [12] remain the same in the presence of this repulsive potential (with the endload λ taken to be the bifurcation parameter).

Assume that we have a branch of critical points $(\mathbf{n}(s;\omega), \mathbf{r}(s,\omega), \theta(s;\omega))$ that satisfy the Euler-Lagrange equations (4.7), plus the boundary conditions $\theta(0) = \theta(1) = 0$ and integral constraint $\int_0^1 \sin(\theta(s))ds = 0$, where ω is introduced to parametrize the branch of solutions. As we have seen, at each value of ω, we are interested in the eigenvalue problem

$$\mathcal{S}h + \mathcal{I}h - cT = \rho h \text{ (for some } c), \quad h(0) = h(1) = 0, \quad \int_0^1 h(s)T(s)\, ds = 0, \qquad (5.1)$$

and in particular in the number of negative eigenvalues ρ at that value of ω.

We want to determine how the eigenvalues ρ change as a fold (a point on the branch of solutions where λ changes direction) is traversed. We begin by demonstrating that the eigenvalue problem (5.1) has a zero eigenvalue $\rho = 0$ at a fold. Differentiating the Euler-Lagrange equations (4.7), the integral constraints, and boundary conditions with respect to ω along the branch yields:

$$\mathcal{S}\dot{\theta} + \mathcal{I}\dot{\theta} - \dot{\lambda}\sin\theta - \dot{\mu}T = 0, \;\; \dot{\theta}(0) = 0, \dot{\theta}(1) = 0, \;\; \int_0^1 \dot{\theta}(s)T(s)\, ds = 0, \tag{5.2}$$

where a dot over a variable indicates differentiation with respect to ω. At a fold (assuming the branch is smooth), we have $\dot{\lambda} = 0$, and in this case, the set of equations (5.2) is equivalent to the eigenvalue problem (5.1) having a zero eigenvalue $\rho = 0$ (with $c = \dot{\mu}$) with corresponding eigenvector $\dot{\theta}$.

Thus, at a fold, $\rho_j = 0$ for some j. Let $h_j(s;\omega)$ be an eigenvector corresponding to the jth smallest eigenvalue in (5.1). For each ω, we can write $\dot{\theta}(s;\omega) = \alpha(\omega)h_j(s;\omega) + \gamma(s;\omega)$ where γ is L^2-orthogonal to h_j. From above, we know that at the fold, $\gamma \equiv 0$.

Now we take the inner product of h_j with the first equation in (5.2):

$$\langle h_j, (\mathcal{S} + \mathcal{I})\dot{\theta}\rangle - \dot{\lambda}\langle h_j, \sin\theta\rangle = 0,$$

where the $\dot{\mu}$ term vanishes since $\langle h_j, T\rangle = 0$ for each ω. From (5.1), we know that $(\mathcal{S} + \mathcal{I})h_j = \rho_j h_j + cT$, and applying this to the equation above (and exploiting the self-adjointness of $\mathcal{S} + \mathcal{I}$), we find:

$$\langle \rho_j h_j + cT, \dot{\theta}\rangle - \dot{\lambda}\langle h_j, \sin\theta\rangle = 0,$$

Using the facts that $\langle T, \dot{\theta}\rangle = 0$ for each ω and $\dot{\theta} = \alpha h_j + \gamma$,

$$\rho_j\alpha = \dot{\lambda}\langle h_j, \sin\theta\rangle.$$

Next we differentiate this with respect to ω:

$$\dot{\rho_j}\alpha + \rho_j\dot{\alpha} = \ddot{\lambda}\langle h_j, \sin\theta\rangle + \dot{\lambda}\frac{d}{d\omega}\langle h_j, \sin\theta\rangle.$$

Evaluating at the fold (where $\rho_j = 0$ and $\dot{\lambda} = 0$):

$$\dot{\rho_j}\alpha = \ddot{\lambda}\langle h_j, \sin\theta\rangle.$$

Multiplying both sides by α and using the fact that $\alpha h_j = \dot{\theta}$ (at the fold):

$$\dot{\rho_j}\alpha^2 = \ddot{\lambda}\langle \dot{\theta}, \sin\theta\rangle = \ddot{\lambda}\int_0^1 \dot{\theta}\sin\theta\, ds.$$

Finally, we note that for any ω,

$$\sin(\theta(s;\omega))\frac{d}{d\omega}[\theta(s;\omega)] = -\frac{d}{d\omega}\cos(\theta(s;\omega))$$

which means that

$$\int_0^1 \sin(\theta(s;\omega))\frac{d}{d\omega}[\theta(s;\omega)] = -\frac{d}{d\omega}\int_0^1 \cos(\theta(s;\omega))ds = -\frac{d}{d\omega}[z(1;\omega)].$$

Thus, at the fold, we have:

$$\dot{\rho_j}\alpha^2 = -\ddot{\lambda}\frac{d[z(1)]}{d\omega}$$

Thus the $(\lambda, z(1))$ bifurcation diagram is "distinguished" in that we can read the sign of $\dot{\rho_j}$ from the shape of the branch in this diagram (at a fold in λ). Specifically, at a fold that opens to the left (so that $\ddot{\lambda} < 0$), the index is one smaller above the fold point than below it (since we can choose to parametrize the branch so that increasing ω corresponds to increasing $z(1)$, and then see that $\dot{\rho_j} > 0$). Similarly, at a fold that opens to the right (so that $\ddot{\lambda} > 0$), the index is one larger above the fold point than below it (since we can choose to parametrize the branch so that increasing ω corresponds to increasing $z(1)$, and then see that $\dot{\rho_j} < 0$).

Acknowledgments. We are very grateful to Andy Salinger at Sandia National Labs for expert assistance with NOX/LOCA and in improving the accuracy and efficiency of the numerics. We also thank Haverford undergraduate research students Lynde Judson, Pat Flanigan, and Ryan Sajac for preliminary computations on the planar rod problem. Finally, we thank John Maddocks and Thomas Seidman for enlightening discussions. R.S.M. was supported by NSF grant DMS-0384739.

REFERENCES

[1] M. S. Birman and M. Z. Solomjak, *Spectral Theory of Self-Adjoint Operators in a Hilbert Space*, D. Reidel Publishing, 1987.

[2] O. Bolza, *Lectures on the Calculus of Variations*, Chelsea Publishing Company, 1973.

[3] B D. Coleman and D. Swigon., *Theory of supercoiled elastic rings with self-contact and its application to DNA plasmids*, J. Elasticity, 60 (2000), pp. 171–221.

[4] G. M. Ewing, *Calculus of Variations with Applications*, Dover Publications, 1969.

[5] I. M. Gelfand and S. V. Fomin, *Calculus of Variations*, Prentice-Hall, 1963.

[6] O. Gonzalez, J.H. Maddocks, F. Schuricht, and H. von der Mosel, *Global curvature and self-contact of nonlinearly elastic curves and rods*, Calc. Var. Partial Diff. Eqns., 14 (2002), pp. 29–68.

[7] S. Goyal, N.C. Perkins, and C.L. Lee, *Nonlinear dynamics and loop formation in Kirchhoff rods with implications to the mechanics of DNA cables*, J. Comp. Phys., (2005).

[8] S. Goyal, N.C. Perkins, and C. L. Lee, *Non-linear dynamic intertwining of rods with self-contact*, Nonlinear Mechanics, 43 (2008), pp. 65–73.

[9] J. Gregory and C. Lin, *Constrained Optimization in the Calculus of Variations and Optimal Control Theory*, Van Nostrand Reinhold, 1992.

[10] M. Heroux, R. Bartlett, V. Howle, R. Hoekstra, J. Hu, T. Kolda, R. Lehoucq, K. Long, R. Pawlowski, E. Phipps, A. Salinger, H. Thornquist, R. Tuminaro, J. Willenbring, A. Williams, and K. Stanley, *An overview of the Trilinos package*, ACM TOMS, 31 (2005), pp. 397–423.

[11] M. R. Hestenes, *Calculus of Variations and Optimal Control Theory*, Robert E. Krieger Publishing Company, 1966.

[12] K. A. Hoffman, *Distinguish bifurcation diagrams for isoperimetric calculus of variations problems and the stability of a twisted elastic loop*, Proc. R. Soc. Lon. A, 461 (2005), pp. 1357–1381.

[13] K. A. Hoffman and T. I. Seidman, *A variational rod model with a singular nonlocal potential.*

[14] T. Kato, *Perturbation Theory for Linear Operators*, Springer-Verlag, Berlin, 1984.

[15] I. Klapper, *Biological applications of the dynamics of twisted elastic rods*, J. Comp. Phys., 125 (1996), pp. 325–337.

[16] J. H. Maddocks, *Stability and folds*, Arch. Rat. Mech. Anal., 99 (1987), pp. 301–328.

[17] R.S. Manning, K.A. Rogers, and J.H. Maddocks, *Isoperimetric conjugate points with application to the stability of DNA minicircles*, Proc. R. Soc. Lon. A, 454 (1998), pp. 3047–3074.

[18] M. Morse, *Introduction to Analysis in the Large*, Institute for Advanced Study, 1951.

[19] R. P. Pawlowski, J. N. Shadid, J. P. Simonis, and H. F. Walker, *Globalization techniques for Newton-Krylov methods and applications to the fully-coupled solution of the Navier-Stokes equations*, SIAM Review, 48 (2006), pp. 700–721.

[20] H. Sagan, *Introduction to the Calculus of Variations*, Dover Publications, 1969.

[21] A.G. Salinger, E.A. Burroughs, R.P. Pawlowski, E.T. Phipps, and L.A. Romero, *Bifurcation tracking algorithms and software for large scale applications*, Int. J. Bif. Chaos, 15 (2005), pp. 1015–1032.

[22] F. Schuricht and H. v.d. Mosel, *Euler-Lagrange equations for nonlinearly elastic rods with self-contact*, Arch. Rational Mech. Anal., 168 (2003), pp. 35–82.

[23] P. Strzelecki and H. von der Mosel, *On rectifiable curves with L^p bounds on global curvature: Self-avoidance, regularity, and minimizing knots*, Math. Z., 357 (2007), pp. 107–130.

[24] D.M. Stump, W.B. Fraser, and K.E. Gates, *The writhing of circular cross-section rods: undersea cables to DNA supercoils*, Proc. R. Soc. Lond A, 454 (1998), pp. 2123–2156.

[25] J.M.T. Thompson, *Stability predictions through a succession of folds*, Phil. Trans. Roy. Soc. London, Series A, Math. and Phys. Sci., 292 (1979), pp. 1–23.

[26] J.M.T. Thompson, G. van der Heijden, and S. Neukirch, *Supercoiling of DNA plasmids: mechanics of the generalized ply*, Proc. R. Soc. Lond A, 458 (2002), pp. 959–985.

[27] I. Tobias, D. Swigon, and B. D. Coleman, *Elastic stability of DNA configurations: I. general theory*, Phys. Rev. E, 61 (2000), pp. 747–758.

[28] G. van der Heijden, S. Neukirch, V.G.A.Goss, and J.M.T. Thompson, *Instability and self-contact phenomena in the writing of clamped rods*, Intl. J. Mech. Sciences, 45 (2003), pp. 161–196.

[29] A. Weinstein and W. Stenger, *Methods of Intermediate Problems for Eigenvalues: Theory and Ramifications*, Academic Press, New York, 1972.

[30] Y. Yang, I. Tobias, and W. K. Olson, *Finite element analysis of DNA supercoiling*, J. Chem. Phys., 98 (1993), pp. 1673–1686.

[31] A. Zettl and Q. Kong, *Eigenvalues of regular Sturm-Liouville problems*, J. Differential Eqns.,

131 (1996), pp. 1–19.